

APPLICATION OF THE VAN DER PAUW STRUCTURE AS
A PIEZORESISTIVE PRESSURE SENSOR – A NUMERICAL STUDY

by

Jesse Townsend Law

A thesis submitted in partial fulfillment
of the requirements for the degree

of

Master of Science

in

Mechanical Engineering

MONTANA STATE UNIVERSITY
Bozeman, Montana

July 2007

© COPYRIGHT

by

Jesse Townsend Law

2007

All Rights Reserved

APPROVAL

of a thesis submitted by

Jesse Townsend Law

This thesis has been read by each member of the thesis committee and has been found to be satisfactory regarding content, English usage, format, citations, bibliographic style, and consistency, and is ready for submission to the Division of Graduate Education.

Dr. Ahsan Mian

Approved for the Department of Mechanical and Industrial Engineering

Dr. Christopher Jenkins

Approved for the Division of Graduate Education

Dr. Carl A. Fox, Vice Provost

STATEMENT OF PERMISSION OF USE

In presenting this thesis in partial fulfillment of the requirements for a master's degree at Montana State University, I agree that the library shall make it available to borrowers under the rules of the library.

If I have indicated my intention to copyright this thesis by including a copyright notice page, copying is allowable only for scholarly purposes, consistent with "fair use" as prescribed in the U.S. Copyright Law. Requests for permission for extended quotation from or reproduction of this thesis in whole or in parts may be granted only by the copyright holder.

Jesse Townsend Law

July 2007

ACKNOWLEDGEMENTS

I would like to thank Dr. Ahsan Mian in his advisory capacity for his advice and guidance on this project among others. I would also like to acknowledge Dr. Douglas Cairns, Dr. Chris Jenkins, and Dr. David Dickensheets for their help and advice as members of my thesis committee. Finally I wish to acknowledge the Montana Space Grant Consortium for partial funding of this work under MSGC grant no. W1128.

TABLE OF CONTENTS

1. INTRODUCTION	1
Stress Measurement	1
Conventional Strain Gage	1
Piezoresistive Strain Gage.....	3
VDP Sensor	5
Pressure Sensing	6
Piezoresistivity.....	7
2. 2D FINITE DIFFERENCE ANALYSIS OF THE VDP	10
Theoretical Development of the VDP as a pressure sensor	10
ϕ Dependence of Normalized Resistance Change Difference	13
Development of Partial Differential Equations	15
Finite Difference Method - Procedure	17
Results and Discussion.....	23
3. 2D FINITE ELEMENT ANALYSIS.....	27
2D ANSYS Model.....	27
Mesh Sensitivity Analysis.....	28
Uniaxial Stress Sensitivity of VDP.....	29
Uniaxial Stress Sensitivity of Serpentine Piezoresistor	30
Summary of Results	34
4. 3D FINITE ELEMENT ANALYSIS.....	35
3D ANSYS Model.....	35
Effect of Stress Stiffening in Diaphragm.....	37
Submodeling.....	37
Pressure Sensitivity of VDP	40
Positional Optimization.....	43
Longitudinal Position Dependence	44
Transverse Position Dependence	45
Angular Alignment Dependence	46
Geometric Optimization.....	47
Size Dependence	48
Depth Dependence	48
Pad Size Dependence	49
Comparison to Analytical Results	50
A Composite VDP Structure	51
The Picture Frame	51
Summary of Results	53

5. CONCLUSIONS.....	55
Experimental Methods (Ongoing Work)	56
REFERENCES CITED	58
APPENDICES.....	60
APPENDIX A: MATLAB ROUTINES	61
APPENDIX B: ANSYS INPUT FILES.....	79
APPENDIX C: MESH DENSITY ANALYSES.....	109
APPENDIX D: CLAMPED PLATE SOLUTION.....	111

LIST OF TABLES

Table	Page
1. Table 1. Boundary condition equations	22
2. Table 2. Piezoresistive properties used in analysis.....	23
3. Table 3. Summary of 2D analysis results	34
4. Table 4. Geometric parameters and material properties.	37
5. Table 5. Analytical stressed diaphragm results	51

LIST OF FIGURES

Figure	Page
1. Typical foil gage geometry	2
2. Typical wheatstone bridge arrangement	3
3. the van der Pauw (VDP) structure.....	5
4. Square diaphragm representation. Stress is measured near diaphragm edge.....	7
5. Diamond cubic crystal structure.....	8
6. Contact Layout on VDP structure	10
7. Axis conventions for following equations.	11
8. Calculated NRCD, to find optimum sensor angle for n- or p-type Silicon. Angle ϕ is relative to the [110] direction on (100) Silicon	15
9. Finite Difference Labeling	18
10. Banded Matrix Structure. Matrix rows correspond to difference equation for nodal numbers.....	20
11. Finite difference solution of VDP potential	23
12. Normalized Resistance Change for n type silicon at 45°	24
13. Normalized Resistance Change for p-type Si at 0°	25
14. NRCD	25
15. VDP mesh	27
16. density analysis for diaphragm at 100kPa and 50 kPa. The maximum diaphragm stress is plotted and the analytical solution for the stress is overlayed.	29
17. Sensitivity of the 2D VDP under uniaxial stress.....	30
18. Serpentine resistor geometries used for determining NRCD.....	32
19. Sensitivity of serpentine resistor pairs with variable number of legs.....	33

LIST OF FIGURES - CONTINUED

Figure	Page
20. SOLID 187 element. a 10 node element that supports anisotropic elasticity.	35
21. 3D Diaphragm Model Geometry. a) Meshed ANSYS model, showing locations of applied boundary conditions, and b) displacement solution (exaggerated) with color indicating stress.....	36
22. Submodeled analysis region and cross-section showing sensor area.....	39
23. Sensitivity of 3D VDP as compared to 2D analyses. Diaphragm pressure required to generate stress.....	41
24. Coordinate system for position analysis. Origin is positioned over edge of diaphragm.....	43
25. Von Mises stress distribution in half diaphragm model at 100kPa.....	44
26. Longitudinal position analysis. The sensitivity of the VDP on a square diaphragm is strongly dependent on position, with a peak at 2.4% offset towards center.....	45
27. Transverse sensitivity analysis. Highest sensitivity is for centered VDP.....	46
28. Angular sensitivity analysis. The VDP is tolerant of angular misalignment of up to 5 degrees, beyond which it drops significantly.	47
29. VDP size sensitivity analysis. The VDP is not strongly dependent on size.	48
30. VDP depth sensitivity. A shallower VDP has higher sensitivity.	49
31. The submodeled picture frame geometry.....	52
32. Comparison of 'Picture Frame' to VDP sensitivity.....	52
33. Circuit and mask layout for characterization of pressure sensors.....	57

LIST OF EQUATIONS

Equation	Page
1. Stress strain relationship.	1
2. Resistance of foil gage resistor.....	2
3. Gage factor definition.	4
4. NRCD of p- and n-type strain gages.....	4
5. Hooke’s law tensor form	8
6. Continuum form of Ohm’s Law	9
7. First order piezoresistive relationship	9
8. Van der Pauw equation for isotropic conductor.....	8
9. Definition of van der Pauw resistance.	10
10. Unstressed VDP resistance.....	11
11. Biaxial stress VDP resistance, 90°.	12
12. Biaxial stress VDP resistance, 0°	12
13. Biaxial strain definition	12
14. Constitutive relationship for piezoresistivity	12
15. Unrotated resistivity matrix.....	12
16. Rotated resistivity matrix.	12
17. Matrix rotation equation.....	13
18. Transformation matrix	13
19. NRCD definition.....	13
20. Continuity equation for current density.	14
21. Electric potential and current density.	16
22. Current density vector.....	16

LIST OF EQUATIONS - CONTINUED

Equation	Page
23. Continuity equation for VDP	16
24. PDE form of continuity for VDP.....	17
25. Finite difference approximations to PDE terms	19
26. Nodal equation for discretized mesh	19
27. Matrix form of simultaneous equations	20

ABSTRACT

This research characterizes a piezoresistive sensor under variations of both size and orientation with respect to the silicon crystal lattice for its application to MEMS pressure sensing. The sensor to be studied is a four-terminal piezoresistive sensor commonly referred to as a van der Pauw (VDP) structure. It is observed that the sensitivity of the VDP sensor is over three times higher than the conventional filament type Wheatstone bridge resistor. With MEMS devices being used in applications which continually necessitate smaller size, characterizing the effect of size and orientation of a VDP structure on the performance of a MEMS pressure sensor is important.

Due to the limitations of anisotropic etching, silicon diaphragms on which the sensors are fabricated must be rectilinear, and most commonly, square. The sensitivity of the VDP stress sensor is affected by misalignment during the etching/diffusion process and by the size of the sensor relative to the size of the underlying pressure diaphragm. Smaller VDP sensors are able to resolve smaller variations in the stress field, but at diminishing size, manufacturing limitations become important. In this study, we characterize the effect of size and orientation on the sensitivity of the VDP sensor to pressure.

In characterizing the effect of relative size and misalignment on the sensitivity of the VDP sensor, a coupled piezoresistive/stress finite element model is developed which simulates the full stress field over the deformed diaphragm in which the VDP is diffused. The change in resistivity of the VDP is then analyzed to predict the sensitivity of the VDP structure. Sensor size, position relative to the diaphragm, and angular misalignment of the VDP were varied to determine a theoretical result for the dependence of VDP output on those parameters. It is determined that the performance of the sensor is strongly dependent only on the longitudinal position of the sensor on the diaphragm, and is relatively tolerant of other errors in the manufacturing process such as transverse position, sensor depth, and orientation angle.

INTRODUCTION

Stress Measurement

Strain measurement is a fundamental experimental technique in mechanics. Strain measurement is also the indirect method by which stress measurements are made. Stress and strain are inextricably linked; strain is the physical phenomenon that gives rise to stress. Uniaxial stress is inferred from strain using the elementary relationship:

$$\sigma = \varepsilon \cdot E \quad (1)$$

where E is the modulus of elasticity, also referred to as Young's Modulus. σ is stress, units of [MPa] and ε is dimensionless strain.

Conventional Strain Gage

A device that is commonly used in material testing is the *extensometer*. The extensometer is intuitively the most direct method of strain measurement. In a uniaxial material test the extensometer is attached at two points to the material sample and measures, via a small dial, or electronically, the change in length between the two points as the test progresses. The extensometer suffers from limitations, including difficulty in application, mechanical complexity and ability to measure strain in only a single direction.

A *strain gage* is in general any device used to measure strain (elastic or inelastic) in a material. A common device is the serpentine strain gage, or foil gage. The foil gage takes advantage of the change in resistance of a metal foil under strain. The typical geometry

of the foil gage is shown in Figure 1. The large pads in the figure are where the resistance measurement is taken, and they are made as large as possible to minimize their contribution to the voltage change. The majority of the ‘sensing’ area is the very narrow wire that doubles back and forth between the electrodes.

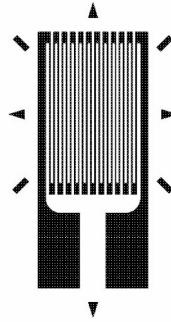


Figure 1. Typical foil gage geometry

The resistance of the foil is given by

$$R = \frac{l \cdot \rho}{A} \quad (2)$$

where l is the length of the resistor, ρ is the resistivity [Ω -cm] and A is the cross sectional area of the resistor. Upon being stressed along the major axis of the foil sensor, the length of the wire increases due to the strain in the underlying material, and the cross sectional area of the resistor is reduced due to the Poisson effect. Under (typically) small strains, the resistance change is typically very small. In practice therefore, foil strain gages are almost always arranged in a wheatstone bridge circuit, which is a resistive voltage divider capable of accurate difference measurement. Moreover, because the gage resistance is

also a function of temperature, the Wheatstone bridge circuit allows temperature compensation of the strain gage. A Wheatstone bridge circuit is shown in Figure 2.

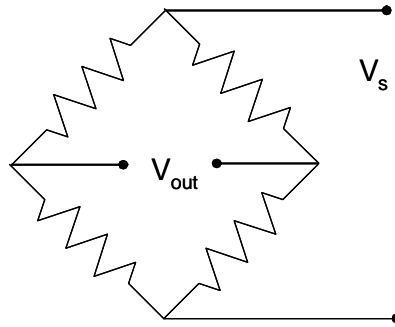


Figure 2. Typical wheatstone bridge arrangement

Piezoresistive Strain Gage

The low sensitivity of the foil strain gage is due to the minor change in geometry of the gage as a result of strain. A gage that changed resistance in direct proportion to stress would have the potential for greater sensitivity, and that is exactly the case for the *piezoresistive strain gage* [1]. Metals typically occur in polycrystalline form and thus exhibit high symmetry in the bulk limit, which is why they exhibit isotropic mechanical and electrical properties. Crystalline solids, however have a regular lattice structure and therefore can exhibit anisotropic material properties. In semiconductor materials, the electrical properties of the bulk solid are a strong function of the band structure of the lattice. In these materials, among which silicon and germanium are the most commonly manufactured, the band structure of the material exhibits dependence on the stress state of the lattice. This is because an applied stress induces a strain in the lattice, which serves to

slightly change the interatomic spacing in the lattice, and thereby asymmetrically change the resistance to flow of electrons in the conduction band.

The net result of this as far as it applies to strain measurement, is that a strain gage manufactured from a piezoresistive material can have a much larger change in resistance for a given strain. The *gage factor* of a strain gage is defined as the normalized resistance change per unit strain:

$$GF = \frac{\Delta R / R_G}{\epsilon} \quad (3)$$

Most foil gages have a gage factor of ~ 2 . A strain gage made of piezoresistive material can have a gage factor ~ 100 [2]. The disadvantages of the piezoresistive strain gage are increased temperature sensitivity, fragility and cost.

However, the piezoresistive gage is incredibly well suited for fabrication directly into the surface of a silicon wafer in microelectronics manufacturing procedures. The resistivity and piezoresistive coefficients of silicon depend on dopant type and concentration, and electrical isolation from the rest of the wafer is achievable using a reverse biased p-n junction. For example, if the silicon wafer is lightly n-type, and the piezoresistor geometry is doped p+, then a diode junction is created at the dopant concentration interface.

For the piezoresistive strain gage, the sensitivity has been determined [3]. For p-type and n-type silicon the maximum sensitivity is given in terms of Normalized Resistance Change Difference (NRCD) given by the equations:

$$\begin{aligned} NRCD_p &= \pi_{44}^p (1 - \nu) \cdot \sigma \\ NRCD_n &= (\pi_{11}^n - \pi_{12}^n)(1 - \nu) \cdot \sigma \end{aligned} \quad (4)$$

where ν is the Poisson's ratio for the material, σ is uniaxial stress, and the π terms are orientation dependent components of the piezoresistive tensor. These equations are presented here for reference; they will be discussed in greater length in following chapters.

VDP Sensor

The van der Pauw (VDP) sensor (Figure 3) is a four-terminal piezoresistive stress sensing structure based on the sheet resistance measurement technique developed by J.J. van der Pauw [4, 5]. The theory has been extended [6, 7] to the analytical solution of a square region of piezoresistive material. The equations allow the calculation of resistance change of the region, given geometry, uniaxial or biaxial stress state, and the piezoresistive coefficients of the material.

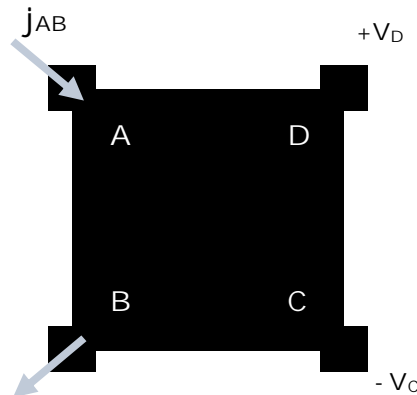


Figure 3. the van der Pauw (VDP) structure

The VDP structure is the primary topic of this thesis work. The theoretical sensitivity has already been established for the use of the VDP sensor in surface stress

measurements. The following analyses treat the details of employing the VDP sensor as a MEMS pressure sensor.

Pressure Sensing

Pressure sensing is a fundamental measurement in many industries. In the automotive industry, for example, a typical passenger car has pressure sensors as part of the powertrain, brake and airbag systems, in tire pressure monitoring, and increasingly in safety and ergonomic systems [8, 9]. In the biomedical industry, pressure sensors find application in invasive and noninvasive monitoring of blood intracranial and epidural pressure as well as in dialysis and other external control systems [10]. Across other industries, pressure sensors are ubiquitous in testing and control.

There are various methods of pressure sensing. For pressure sensing in air, the most common methods are listed below.

1. Capacitive pressure sensors. These sensors typically have one fixed and one flexible conductive plate, which flexes when subjected to pressure. The capacitance between the plates changes as a function of their proximity, which in turn is a function of the pressure. These sensors can also be micromachined from silicon.
2. Resonance pressure sensors. These sensors exploit a vibrating element, often a cantilever or cylinder. The air pressure changes the resonance properties of the structure due to structural deformation or to air friction, and the shift in resonant frequency is measured electrically or optically and correlated to pressure

3. Optical pressure sensing. Optical pressure sensors use laser displacement sensors to measure nanometer scale deflection of a diaphragm surface that displaces under pressure.
4. Strain gage based sensing. As discussed above, this uses a strain gage sensor on a diaphragm infer stress on the diaphragm surface, which can then be correlated to diaphragm pressure.
5. Piezoresistive strain sensing. This device also measure strain on the surface of a pressure diaphragm, but uses a diaphragm of piezoresistive material, and exploits the piezoresistive effect of the gage to achieve substantially higher sensitivity.

The VDP sensor as explored in this paper is of the last type of pressure sensor listed above. For ease of manufacturing with conventional manufacturing methods, the diaphragm is square. A representation of the diaphragm is shown in Figure 4 below.

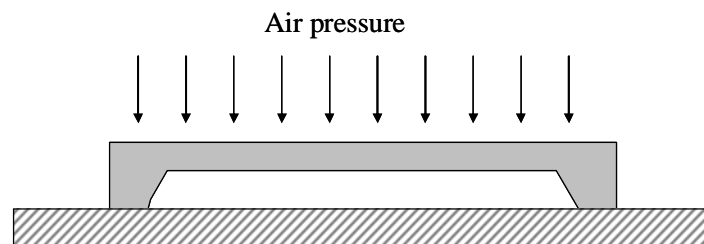


Figure 4. Square diaphragm representation. Stress is measured near diaphragm edge.

Piezoresistivity

Piezoresistivity in silicon was first described by Smith [11] in 1954. Phenomenologically, piezoresistance is a change in resistance due to material strain.

Although most or all materials exhibit some degree of piezoresistivity, it is consequential and of engineering interest in far fewer materials. The most common of these materials is single crystal silicon, although polycrystalline silicon also exhibits the effect [12]. Single crystal silicon has a Diamond cubic structure as shown in Figure 5.

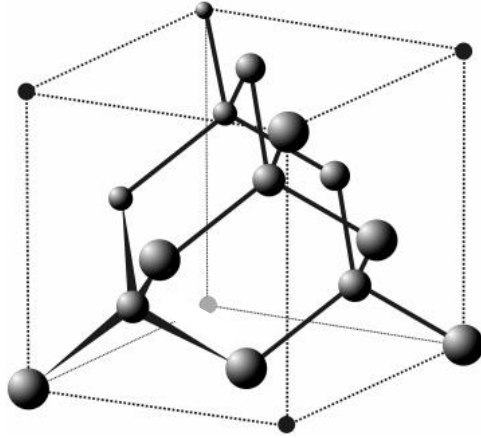


Figure 5. Diamond cubic crystal structure.

Stress applied to a piezoresistive material, such as silicon, results in material strain. In general, the relationship between stress and strain can be of any form. For single crystal silicon however, assuming a Hookian relationship is appropriate. The relationship between stress and strain can be written as

$$\sigma_{ij} = E_{ijkl} \epsilon_{kl} \quad (5)$$

where E_{ijkl} are components of the elastic modulus tensor. Here indicial notation is used and the subscripts i,j,k,l take values 1,2,3 corresponding to x,y,z directions.

The resulting strain in the material changes the interatomic spacing between silicon atoms (and doped impurities), which in turn changes the electronic potential locally experienced by the electrons. Charge conduction in silicon is determined by the

concentration or dopant atoms which influence the band gap between the valence and conduction energy bands. The change in local potential seen by the electrons modifies this energy gap, increasing or decreasing the conductivity of silicon lattice in a directionally dependent manner. The relationship between electric field strength and current density in a conductor without the piezoresistance effect is given by

$$\bar{E}_i = \rho_{ij} J_j \quad (6)$$

here the Greek capital epsilon with overbar, \bar{E} , denotes electric field strength [V/cm], and is distinguished from Young's modulus. ρ is the resistivity tensor [Ω -cm], J is the current density [A/cm^2]. Incorporating first order piezoresistivity changes the form of the above equation to the following:

$$\bar{E}_i = \rho_{ij} [I_{jk} + \Pi_{jklm} \sigma_{lm}] J_k \quad (7)$$

where Π is the piezoresistivity tensor and I is the 2nd rank idem tensor.

Due to the high symmetry of the silicon lattice, most of the components of both the elastic modulus and piezoresistive tensors are zero or repeated. After symmetry considerations there are only 3 remaining components of each of the aforementioned tensors. The published values of the elastic modulus coefficients [13], and the piezoresistive coefficients [11] are listed in Table 4.

2D FINITE DIFFERENCE ANALYSIS OF THE VDP

Theoretical Development of the VDP as a pressure sensor

Van der Pauw's theorem for an isotropic conductor [4, 5] states:

$$\exp\left(-\frac{\pi t R_{AB,CD}}{\rho}\right) + \exp\left(-\frac{\pi R_{BC,DA}}{\rho}\right) = 1 \quad (8)$$

Here t is the thickness of the conductor, ρ is the isotropic resistivity, and the "Resistance" $R_{AB,CD}$ is defined as the potential difference $V_D - V_C$ per unit current through contacts A and B. This is illustrated in Figure 6 below.

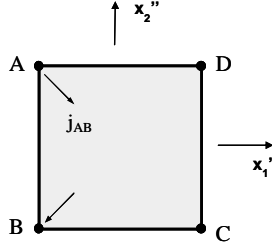


Figure 6. Contact Layout on VDP structure

Similarly, the "Resistance" $R_{BC,DA}$ as the potential difference $V_A - V_D$ per unit current through contacts B and C, or:

$$R_{AB,CD} = \frac{V_D - V_C}{j_{AB}}, R_{BC,DA} = \frac{V_A - V_D}{j_{BC}} \quad (9)$$

For a rotationally symmetric structure, such as the proposed VDP structure, the terms $R_{BC,DA}$ and $R_{AB,CD}$, in Eqn. (8) are equal, and that equation can be expressed as an analytical solution of the unstressed resistance:

$$R_{AB,CD} = R_{AD,BC} = \frac{\rho \ln 2}{\pi t} \equiv R^0 \quad (10)$$

The unstressed resistance will be used to normalize the resistance change for a stressed VDP conductor.

The axis labeling conventions are shown relative to a silicon wafer as in Figure 7 below. The wafer depicted is a [100] wafer, and the crystallographic axes are designated x_1 and x_2 . The primed axes, x_1' and x_2' , are oriented at 45° to the crystallographic axes, and angle of rotation, ϕ , of the VDP sensor are in reference to the primed coordinates. The double-primed coordinate system shares an origin with the unprimed and primed coordinate system, but is rotated by ϕ with respect to the primed coordinates. All of the analyses in this research are based on [100] silicon.

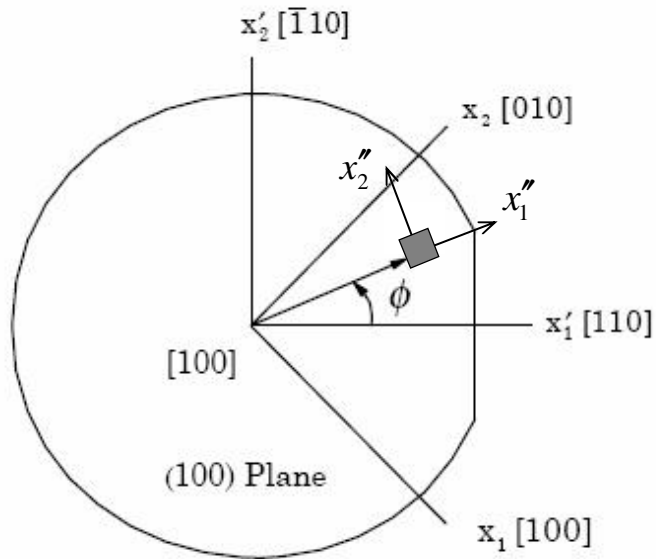


Figure 7. Axis conventions for following equations.

The resistance equations for a square VDP sensor under biaxial stress conditions are given by [6],

$$R_{AD,BC} = R_{\varphi+90}^{\sigma} = -\frac{8\sqrt{\rho''_{11}\rho''_{22}}}{\pi t} \ln \prod_{n=0}^{\infty} \left\{ \tanh \left[\frac{AB}{CD} \sqrt{\frac{\rho''_{11}}{\rho''_{22}}} (2n+1) \frac{\pi}{2} \right] \right\} \quad (11)$$

$$R_{AB,CD} = R_{\varphi}^{\sigma} = -\frac{8\sqrt{\rho''_{11}\rho''_{22}}}{\pi t} \ln \prod_{n=0}^{\infty} \left\{ \tanh \left[\frac{CD}{AB} \sqrt{\frac{\rho''_{22}}{\rho''_{11}}} (2n+1) \frac{\pi}{2} \right] \right\} \quad (12)$$

where the double primed ρ values represent the components of the resistivity tensor in the rotated system, and AB and CD are the deformed dimensions such that

$$\frac{AB}{CD} = \frac{1 + \varepsilon''_{11}}{1 + \varepsilon''_{22}} \quad (13)$$

The principal resistivity components, ρ''_{11}, ρ''_{22} , are calculated from the general constitutive relationship for piezoresistivity:

$$\rho_{ik}^{\sigma} = \rho_{ij}^0 \left[I_{jk} + \Pi_{ijkl} \sigma_{lm} \right] \quad (14)$$

where Π is the 4th rank piezoresistivity tensor. Due to the cubic symmetry of the silicon lattice, only three independent piezoresistivity values remain: π_{11} , π_{12} , and π_{44} [4]. Additionally, because we are considering only 2-D planar stress states, we assume that the stress tensor has only 3 independent values, σ_{11} , σ_{22} , and σ_{12} . Employing reduced tensor notation, the equations can be simplified, such that ρ and σ are represented as 3-element vectors, and Π is a 3x3 matrix. The equation then becomes:

$$\mathbf{\rho}^{\sigma} = \rho^0 \left[\begin{bmatrix} 1 \\ 1 \\ 0 \end{bmatrix} + [\Pi] \bullet \mathbf{\sigma} \right] \quad (15)$$

The values of ρ''_{11}, ρ''_{22} can be calculated from the equivalent equation in the double-primed (sensor) coordinate system:

$$\rho''_{\sigma} = \rho^0 \left[\begin{array}{c} 1 \\ 1 \\ 0 \end{array} \right] + [\Pi''] \cdot \sigma'' \quad (16)$$

where

$$[\Pi''] = [T] \cdot [\Pi] \cdot [T]^{-1} \quad (17)$$

with T a transformation matrix defined such that:

$$\begin{aligned} \rho''_{\sigma} &= [T] \cdot \rho^{\sigma} \\ \sigma'' &= [T] \cdot \sigma \end{aligned} \quad (18)$$

$$[T] = [T(\theta'')] = [T(\varphi + 45^{\circ})]$$

Here θ'' is the angle from unprimed coordinates ([100] silicon axis) to the double primed coordinates (VDP sensor). The same formulation is used for the calculation of strains from the applied stress state. E, the elasticity tensor is similarly reduced due to crystal symmetry and the coordinate transform is performed as above

φ Dependence of Normalized Resistance Change Difference

The stress state of a VDP sensor for a given circular diaphragm pressure is independent of angle φ , because to a good approximation such a diaphragm has only radial and tangential stresses. However, in the sensor coordinate system, the piezoresistivity components depend on φ , as seen in eq. (18). In this analysis, the angle φ which yields a theoretical maximum sensitivity is determined. Two types of silicon: p-type and n-type were considered by a suitable change in piezoresistivity coefficients [11]

in the equations. Eqs. (11-18) were used to calculate the “Normalized Resistance Change Difference”, (NRCD), given by:

$$NRCD = \Delta R_{\varphi} - \Delta R_{\varphi+90^{\circ}} = \frac{R_{\varphi}^{\sigma} - R_{\varphi}^0}{R_{\varphi}^0} - \frac{R_{\varphi+90^{\circ}}^{\sigma} - R_{\varphi+90^{\circ}}^0}{R_{\varphi+90^{\circ}}^0} \quad (19)$$

As shown in [7], this quantity is a desirable measure of sensitivity because it is temperature compensated.

The results of the calculations are presented in Figure 8. It can be seen that maximum NRCD is obtained at $\varphi = 0^{\circ}$ or 90° for p-type silicon, and at $\varphi = 45^{\circ}$ for n-type silicon. Furthermore, the maximum NRCD for n-type silicon is 8.8% greater than for p-type silicon. Qualitatively, this behavior is identical for all biaxial stress states. Quantitatively, however, the results are for the stress at the edge of a 20 μm thick, circular diaphragm with diameter 1000 μm under a pressure of 100 kPa.

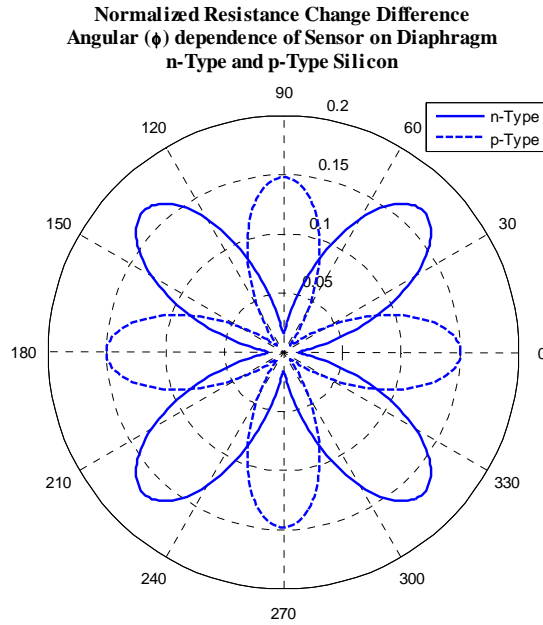


Figure 8. Calculated NRCD, to find optimum sensor angle for n- or p-type silicon.

Angle ϕ is relative to the $[110]$ direction on (100) silicon

With the above sensitivity results, the scope of the numerical analysis is reduced, as p-type sensors will be only analyzed at an angle of 0° to the x_1' ($[110]$) axis, and n-type sensors will be analyzed only at an angle of 90° to the x_2' $[110]$ axis.

Development of Partial Differential Equations

In order to establish the ability to simulate VDP structures numerically and to support the analytical results for the VDP sensitivity, the 2D VDP structure was simulated using MATLAB. The scope of the MATLAB simulation was to first establish the governing equations for the flow of current through an anisotropic conductor, to derive a partial differential equation, and finally to approximate the solution to that equation using a finite difference method.

The first assumption used in modeling the VDP behavior was of steady state behavior. We want only to know the steady state behavior of the structure; therefore there will be no charge accumulation and we can write the continuity equation for the current density, J , as

$$\frac{\partial J_1''}{\partial x_1''} + \frac{\partial J_2''}{\partial x_2''} = 0 = \frac{\partial J_i''}{\partial x_i''} \quad (20)$$

where the common indicial notation will be employed to indicate summation over repeated indices. The electric field strength, \bar{E} , at any point can be expressed as a derivative of the electric potential, V , and furthermore as the tensor product of the resistivity and the current density.

$$\bar{E}_i'' = -\frac{\partial V}{\partial x_i''} = \rho_{ij}'' J_j'' \quad (21)$$

Inverting this equation to solve for the current density vector, and defining the conductivity tensor κ'' , as the inverse of the resistivity tensor

$$J_i'' = -(\rho_{ij}'')^{-1} \frac{\partial V}{\partial x_j''} = -\kappa_{ij}'' \frac{\partial V}{\partial x_j''} \quad (22)$$

Substituting Eqn. (20) into Eqn. (22) yields

$$\frac{\partial}{\partial x_i''} \left(\kappa_{ij}'' \frac{\partial V}{\partial x_j''} \right) = 0 \quad (23)$$

which is the steady state assumption cast in terms of a continuity equation for current density, with voltage as the dependent variable. For clarity, Eqn. (23) is expanded:

$$\kappa_{11}'' \frac{\partial^2 V}{\partial x_1''^2} + 2\kappa_{12}'' \frac{\partial^2 V}{\partial x_1'' \partial x_2''} + \kappa_{22}'' \frac{\partial^2 V}{\partial x_2''^2} = 0 \quad (24)$$

Eqn (24) is a partial differential equation, whose structure depends on the values of the conductivity tensor. The conductivity tensor, κ , has the structure $\begin{bmatrix} \kappa_{11} & \kappa_{12} \\ \kappa_{12} & \kappa_{22} \end{bmatrix}$. The general second order linear differential equation in two independent variables has the form $Au_{xx} + 2Bu_{xy} + Cu_{yy} + Du_x + Fu_y + Gu + H = 0$, where $u = u(x,y) = V(x,y)$ and subscripts indicate partial derivatives in the independent variables. Therefore the sign of determinant of the reduced conductivity matrix, as given above determines the class of the partial differential equation in (24). For silicon, it is the case that the equation is always elliptic, i.e. $\kappa_{12}^2 - \kappa_{11}\kappa_{22} < 0$. This condition ensures diagonal dominance of the finite difference matrix that will be constructed, and therefore ensures convergence of iterative solution routines.

Finite Difference Method - Procedure

After having established the equation to be solved and the ellipticity of the equation, it remains to discretize the VDP region and develop the applicable difference equations. Reference [14] develops the difference equation for this second order PDE, but before presenting the equations, it serves well to establish the notation that will be used to represent the geometric positions of point in the mesh. In general a good method of representing the discretized points, is by using indicial subscripts. For example a point would be represented by $u_{i,j,k}$ in three dimensions or $u_{i,j}$ in two dimensions. The i and j

subscripts represent position in the x- and y- directions, respectively. For any point $u_{i,j}$, the point adjacent in x is $u_{i+1,j}$ and the point adjacent in increasing y is $u_{i,j+1}$. This notation lends itself well to dimensional generalization and especially to implementation in computer code, where the finite difference matrix is developed iteratively, and the subscripts lend naturally to looping structures.

However for the sake of intuitive clarity, an alternate notation will be presented in the present discussion. Since we are currently limited to a 2D discussion, it is clearer to develop the finite difference *molecule* using compass directions. The notation of the mesh grid is illustrated in Figure 9.

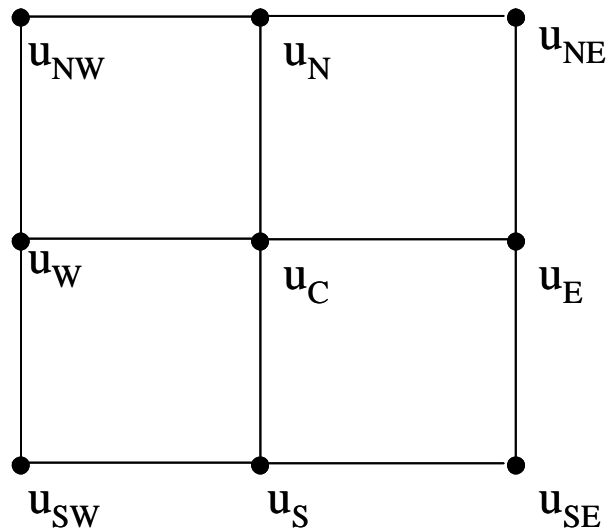


Figure 9. Finite Difference Labeling

Now the partial derivatives in Eqn. (24) can be replaced as follows:

$$\begin{aligned}
\frac{\partial^2 u}{\partial x_1^2} &= \frac{1}{h^2} (u_E - 2u_C + u_W) \\
\frac{\partial^2 u}{\partial x_1^2} &= \frac{1}{h^2} (u_N - 2u_C + u_S) \\
\frac{\partial^2 u}{\partial x_1 \partial x_2} &= \frac{1}{4h^2} (u_{NE} - u_{NW} + u_{SW} - u_{SE})
\end{aligned} \tag{25}$$

The last of the equations can be chosen differently as discussed in [14], but for this case, where the partial derivatives are multiplied by conductivity, this form is sufficient to ensure that a diagonally dominant matrix is obtained. Furthermore, for this form, the truncation error can easily be shown to be of order $O(h^2)$. The full equation for a given mesh point then is

$$\kappa_{11} (u_E - 2u_C + u_W) + \kappa_{12} \frac{1}{4} (u_{NE} - u_{NW} + u_{SW} - u_{SE}) + \kappa_{22} (u_N - 2u_C + u_S) = 0 \tag{26}$$

This equation then must be solved implicitly for every node in the mesh. There will be one such equation for every node in the mesh. If the mesh has 20 subdivisions in x and y, this corresponds to the simultaneous solution of 400 equations. The system of equations is put into matrix form, wherein the nodal matrix is of dimension 400 x 400, for a total of 160,000 matrix elements. For this reason, dense meshes quickly become unmanageably large. An example of the nodal matrix for a 4x4 nodal mesh is shown in Figure 10. In the equation matrix only the subscript has been used to indicate that the matrix entry should correspond to the weight factor of the voltage value for the node in the direction indicated by the subscript. For example, the entry SW in matrix row 3, indicates that the matrix element should be filled with the weighted value of the voltage at the node to the Southwest of Node 3, in this case the Voltage value at node 6. It is clear

value in the $\{x\}$ solution vector. A Neumann boundary condition is equivalent to specifying the current flow, and is the method used in this model. A Neumann boundary condition is applied at all boundary nodes, simulating no current flow at the boundary. The only exception is at the corner nodes at which a ‘voltage’ is applied. At these nodes, Neumann boundary conditions are specified to model the effect of current flow through the sensor. The applied voltage resulting from the forced current is then measured at the end of the solution procedure. This method is easier to implement than use of Dirichlet conditions to specify applied voltage.

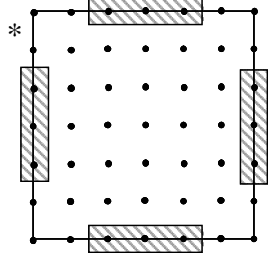
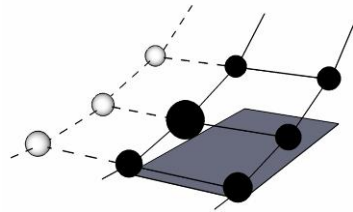
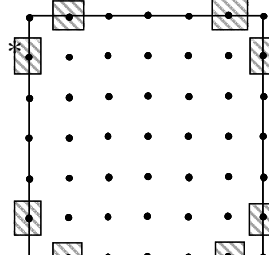
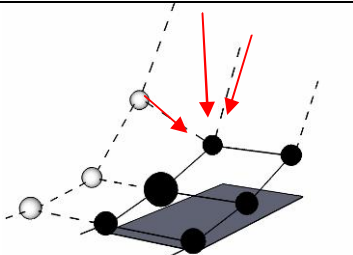
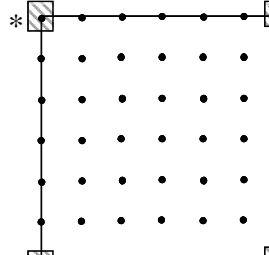
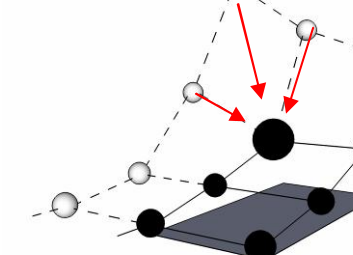
The situation is actually somewhat more complicated than this; application of the Neumann conditions requires updating the nodal equation matrix, so the missing entries indicated by $\underline{0}$ are actually added to the opposite cardinal direction. This has the effect of causing the derivative at the boundary to be zero, which is what is desired. The details of the matrix construction are not particularly illuminating, but for completeness the boundary condition equations are listed below. The equations given in Table 1 include the weighting factors that are applied to the nodes. These weighting factors depend on the form of the difference equation chosen and include the effect of negative values. For details see reference [14]. In the nodal diagram in the table, the height of the nodes above the grey planar surface represents the voltage at that node for a typical solution. Filled nodes and solid lines represent physical areas of the mesh, while unfilled nodes and dashed lines represent ‘virtual’ nodes that are used to visualize the boundary conditions. By fixing the height of a virtual node at the same voltage value as the real node at a position mirrored across the boundary the condition $\frac{\partial V}{\partial x_i} = 0$ is enforced, which is

equivalent to an insulated boundary normal to the i direction. Similarly, by enforcing

$\frac{\partial V}{\partial x_i} = C$, where C is a constant, a fixed current flow through boundary nodes can be

imposed.

Table 1. Boundary condition equations

Boundary Position	Condition	Application Region	Nodal Diagram
Side	Insulated Boundary		
Eqn (*)			$M_N u_N + (M_{NW} + M_{NE}) u_{NE} + M_{CuC} + (M_W + M_E) u_E + M_S u_S + (M_{SW} + M_{SE}) u_{SE} = 0$
Corner Adjacent			
Eqn (*)			$M_N u_N + (M_{NE} + M_{NW}) u_{NE} + M_{CuC} + (M_E + M_W) u_E + M_S u_S + (M_{SE} + M_{SW}) u_{SE} = 2h V_X M_{NE}$
Corner	Forced Current		
Eqn (*)			$M_{CuC} + (M_E + M_W) u_E + (M_N + M_S) u_S + (M_{NW} + M_{NE} + M_{SW} + M_{SE}) u_{SE} = 2h [V_X (M_{NW} + M_W) + V_Y (M_{NW} + M_N)]$

Results and Discussion

The model is solved iteratively using MATLAB's built in least squares solver, *lsqr.m*, and a voltage solution is obtained. A representative surface plot of the solution is shown in Figure 11. The material properties used in the analysis are taken from the literature [11] and are reproduced in Table 2. The geometric properties of the VDP for the 2D MATLAB simulation are a VDP size of $100\mu\text{m} \times 100\mu\text{m}$, with thickness of $20\mu\text{m}$. A 41×41 nodal mesh was used in obtaining the results that follow.

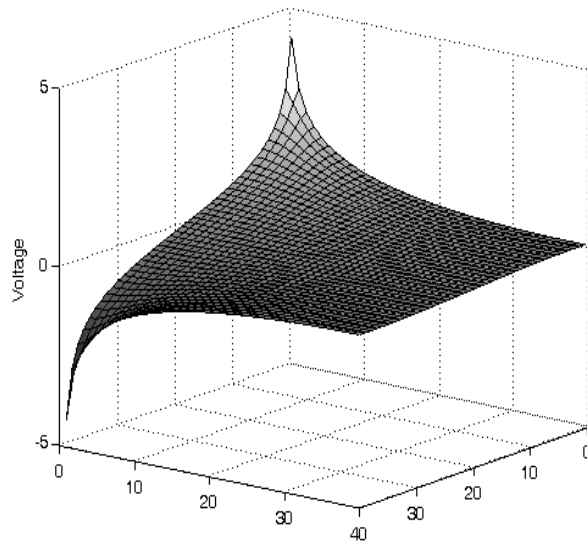


Figure 11. Finite difference solution of VDP potential

Table 2. Piezoresistive properties used in analysis

Type	Resistivity	π_{11}	π_{22}	π_{44}
Units	$\Omega\text{-cm}$	10^{-11} Pa^{-1}	10^{-11} Pa^{-1}	10^{-11} Pa^{-1}
p-type	7.8	6.6	-1.1	138.1
n-type	11.7	-102.2	53.4	-13.6

The simulated “Resistance” of the VDP, as provided in Eqn. (9) is obtained from the finite difference model by measuring the voltage at points D and C, and dividing the difference into the current which we applied to the model. In order to calculate the Normalized Resistance Change (NRC), a biaxial stress that would occur on a circular diaphragm is calculated. This stress is used to calculate the resistivity tensor, using the transformation in Eqn. (14). The resistivity matrix is then rotated using a matrix transformation as in Eqn (18) to either a 0° or 90° rotation. The resistance of the sensor is obtained as a function of increasing biaxial stress (proportional to diaphragm pressure in the small deflection limit). The results of the calculations are given in Figure 12 through Figure 14. In Figure 12 and Figure 13, NRC is plotted as a function of Biaxial Stress Difference, defined as $\sigma_{rr} - \sigma_{\theta\theta}$, where σ_{rr} is the diaphragm stress in the radial direction, and $\sigma_{\theta\theta}$ is the stress in the tangential direction. Figure 12 gives the results for n-type silicon, Figure 13 gives the results for p-type silicon.

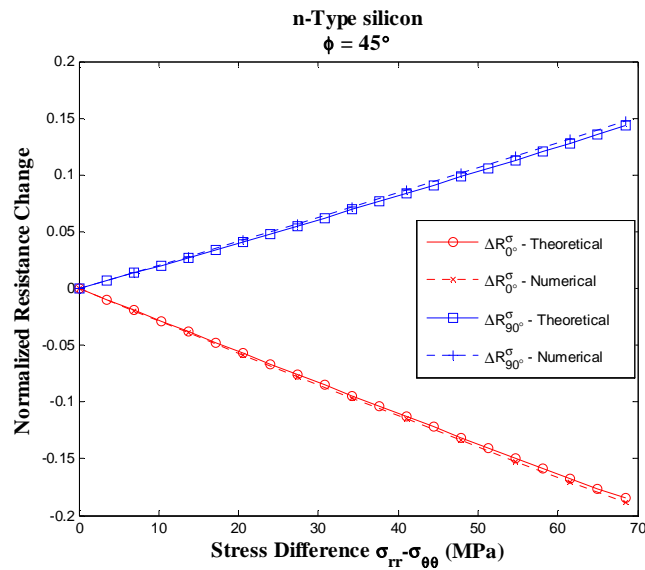


Figure 12. Normalized Resistance Change for n type silicon at 45°

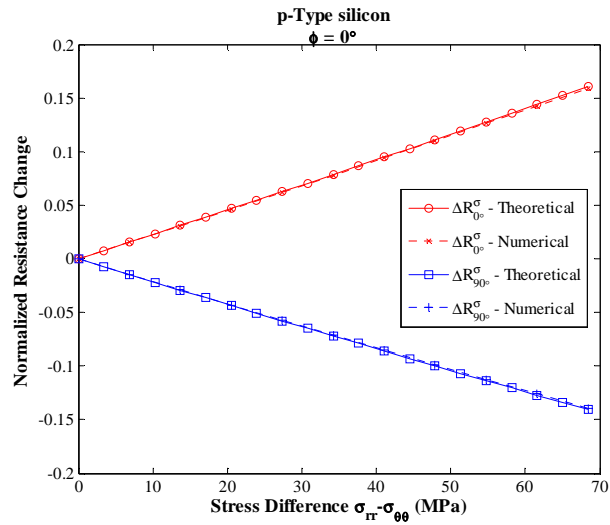


Figure 13. Normalized Resistance Change for p-type Si at 0°

For each of the two figures above the NRCD is calculated by subtracting the two sensitivity curves (although linear) and the p-type and n-type based sensors are compared in Figure 14.

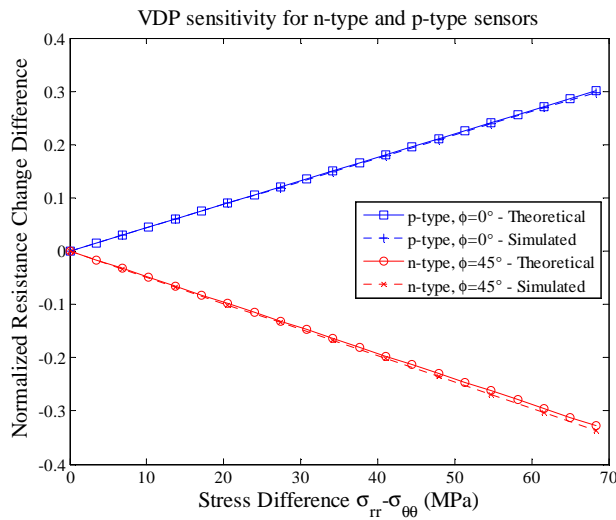


Figure 14. NRCD

It can be seen in Figure 12-Figure 14 that the agreement between the theoretical VDP sensitivity (calculated from Eqns. 9-19) and the sensitivity as calculated using the MATLAB based finite difference method is excellent. There is a slight deviation between the two methods which is likely the result of a shortcoming in the MATLAB finite difference implementation in which nodal spacing is not allowed to vary to remain consistent with the calculated strain conditions. Since we are operating in the small strain limit, this is not cause for concern in light of the accuracy of the results. Additionally, the biaxial stress calculations are based on an isotropic circular diaphragm, while silicon has anisotropic elastic modulus. Poisson's ratio as used in the biaxial stress calculation serves as an easily calculated approximation to the anisotropic strain response of the silicon.

These approximations aside, the MATLAB results are sufficiently accurate for further investigation into the behavior of the VDP sensor, and serve as a starting point for the Finite Element Analysis (FEA) modeling that follows.

2D FINITE ELEMENT ANALYSIS

2D ANSYS Model

2D finite element models of the piezoresistive structures were created in ANSYS Multiphysics 10.0 [15]. ANSYS is used for the rest of the simulations discussed in this paper. The 2D models are based on the example FTT piezoresistive analysis in the coupled-field analysis guide in the ANSYS documentation.

The VDP model is shown in Figure 15, and consists of a small region of material in which the doped VDP structure is embedded. The input file for the analysis is provided in Appendix C. The background material is modeled with Element type PLANE183, a plane stress structural element. The central region is meshed with Element type PLANE223, a coupled field element with voltage degree of freedom. The model is solved for the NRCD as in Eqn. 19.

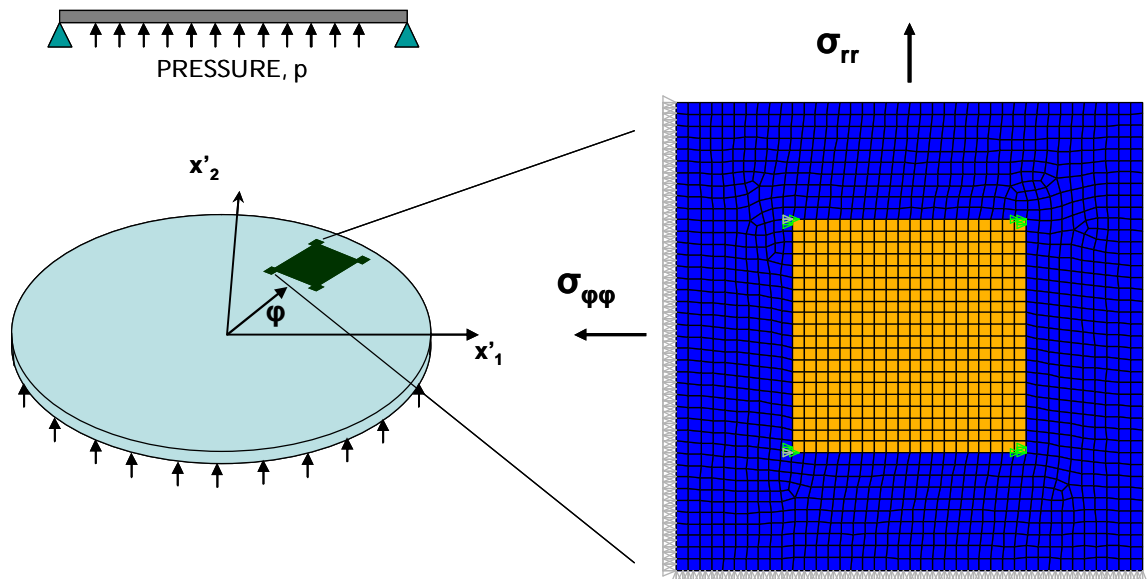


Figure 15. VDP mesh

Pressure is applied as a surface force on the right boundary of the meshed region, and the model is constrained at the left and bottom edges. The voltage DOF is specified at the upper left and lower left corners as +5 V and +0 V respectively. Additionally, the input and output voltages are specified over a small square of nodes to approximate the connection that would physically occur if this device were connected by a via. The model is first solved in an unstressed state and subsequently solved in a stressed state. In the stressed state the ‘Resistance’ is obtained for both 0° and 90° orientations. The ‘Resistance’ is calculated by mapping the current vector solution onto a path object that defines cross-section of the VDP structure and then integrating the mapped data along the length of the path. The element current vector solution is decomposed into components normal and tangential to the cross section of the VDP. These mappings are then integrated over the surface and finally summed in a vector sense. The 2D elements in this model have a default thickness of 1 unit, so the integrated current value is multiplied the thickness of the VDP, to obtain the resistance in a VDP with depth.

Mesh Sensitivity Analysis

For each of the 2D structure models, the sensitivity of the results on the number of elements is investigated to ensure the solution is decoupled from the mesh density. For the VDP structure the mesh sensitivity analysis is presented in Figure 16. It can be seen that beyond 64 elements, the results do not depend on mesh density. A mesh density of 400 elements was selected for the analysis, as this density gave good contour plots while still solving quickly.

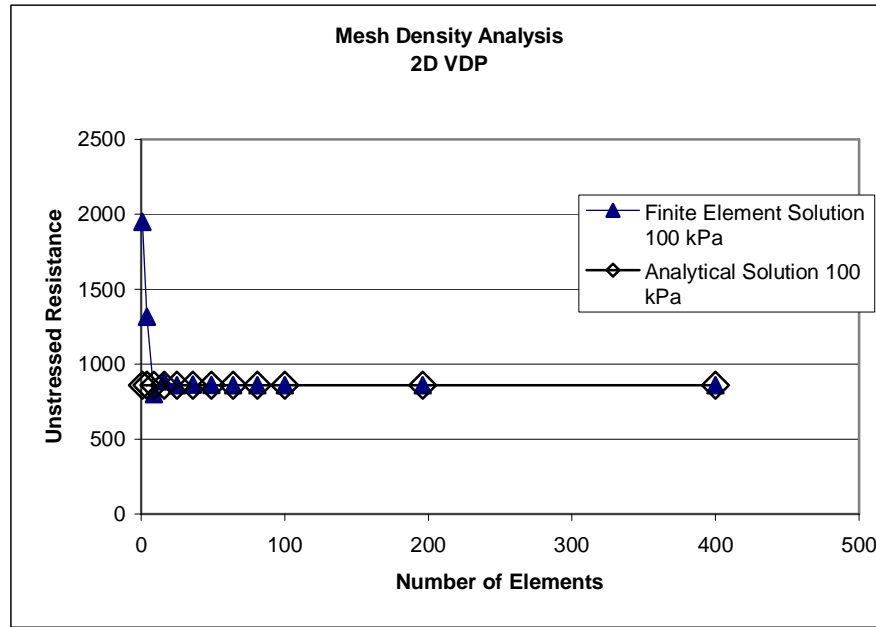


Figure 16. density analysis for diaphragm at 100 kPa and 50 kPa. The maximum diaphragm stress is plotted and the analytical solution for the stress is overlaid.

This provides evidence that the model is giving precise results, although the accuracy of those results is dependent on the model having been structured properly. The mesh density analysis is also presented in Appendix C. Subsequent analyses are presented solely in Appendix C.

Uniaxial Stress Sensitivity of VDP

The pressure sensitivity of the 2D VDP model is given in units of $[\text{mV}(\text{out})/\text{V}(\text{in})/\text{MPa}]$ or more conveniently as GPa^{-1} . The data presented in Figure 17 shows the sensitivity of the 2D VDP sensor to uniaxial stress. The sensitivity of the 2D

sensor to Uniaxial stress is 4.35 GPa^{-1} which matches the theoretical value within about 1%.

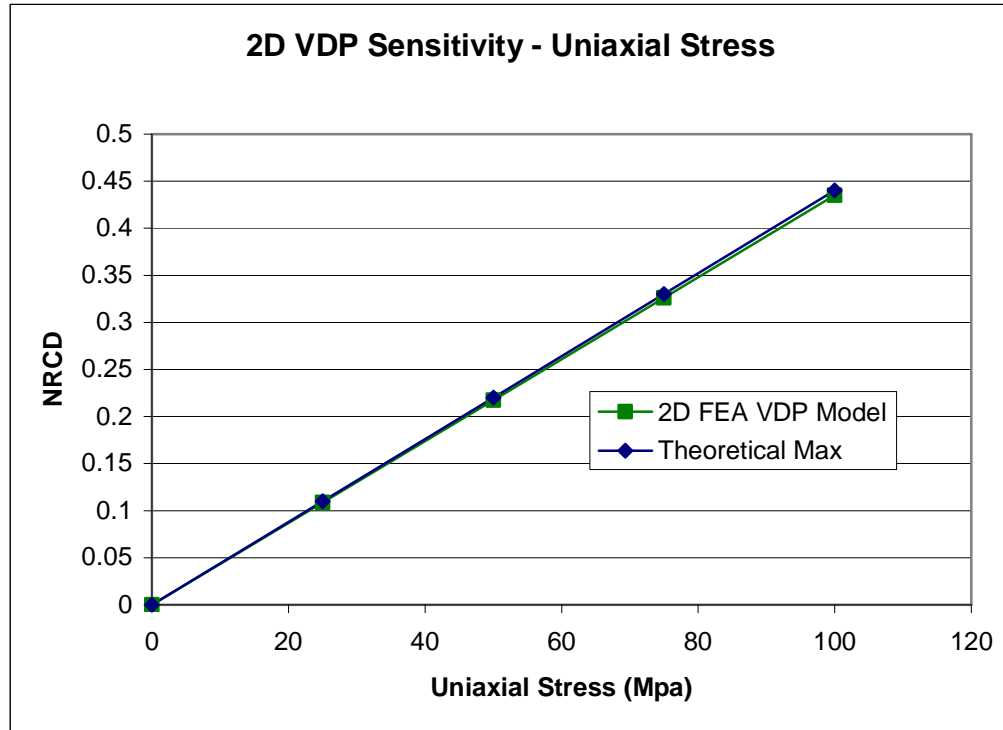


Figure 17. Sensitivity of the 2D VDP under uniaxial stress.

The sensitivity of the VDP is linear, which is unsurprising, since there are no nonlinearities incorporated into the material model. This is justifiable based on the fact that we are staying well below the elastic limit for silicon, a brittle material, and because nonlinearities in the piezoresistive coefficients are necessarily empirical.

Uniaxial Stress Sensitivity of Serpentine Piezoresistor

In the previous section, the NRC D of the VDP under uniaxial stress was determined with a 2D FEA model. To compare the NRC D of the VDP with the serpentine

piezoresistor, the piezoresistor was modeled in different configurations (Figure 18) and the NRCD was calculated as in Eqn. (19). In order to calculate the NRCD and establish a basis of comparison between the two terminal measurement of the serpentine resistor and the VDP, for each serpentine resistor geometry, two geometries were actually calculated. Uniaxial stress was applied to the model for a resistor in both the 0° and 90° orientations with respect to the direction of applied stress. The NRCD was then calculated, providing an equivalent, temperature compensated sensitivity measure. The serpentine resistor geometries considered were those with 4, 6, 8, and 16 legs. In Figure 18, the 0° orientation is shown. The width of the 'legs' was allowed to vary, although the interconnect widths were held constant. No further geometries beyond those shown were analyzed, and the effect of varying interconnect size was not considered.

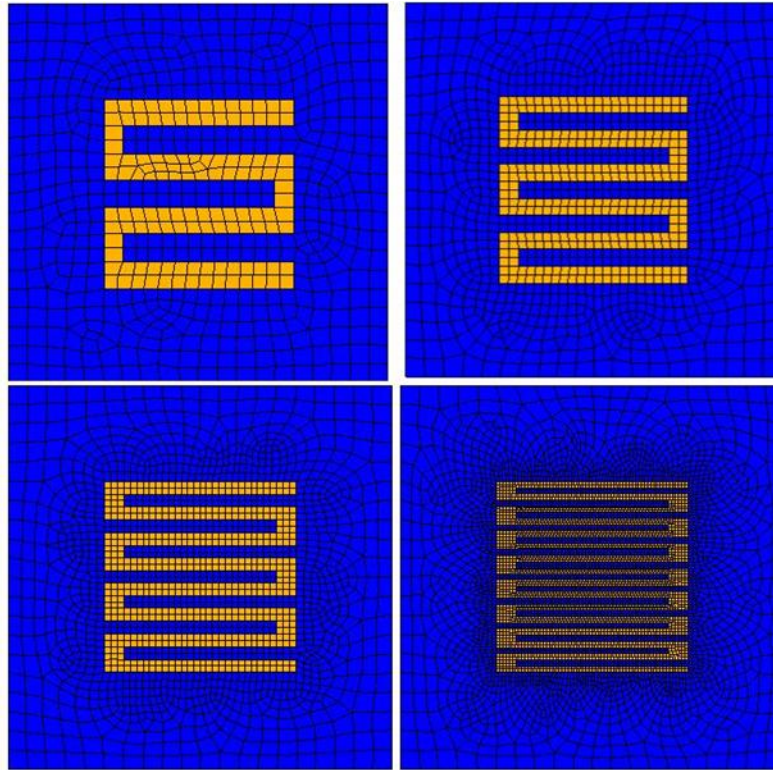


Figure 18. Serpentine resistor geometries used for determining NRCD

The results of the FEA analysis are presented in Figure 19. The results are compared to the theoretical value [3]. It can be inferred from the figure, that as the number of legs increases, the sensitivity of the serpentine resistor pair approaches the theoretical value of 1.381 GPa^{-1} as predicted in Eqn (4).

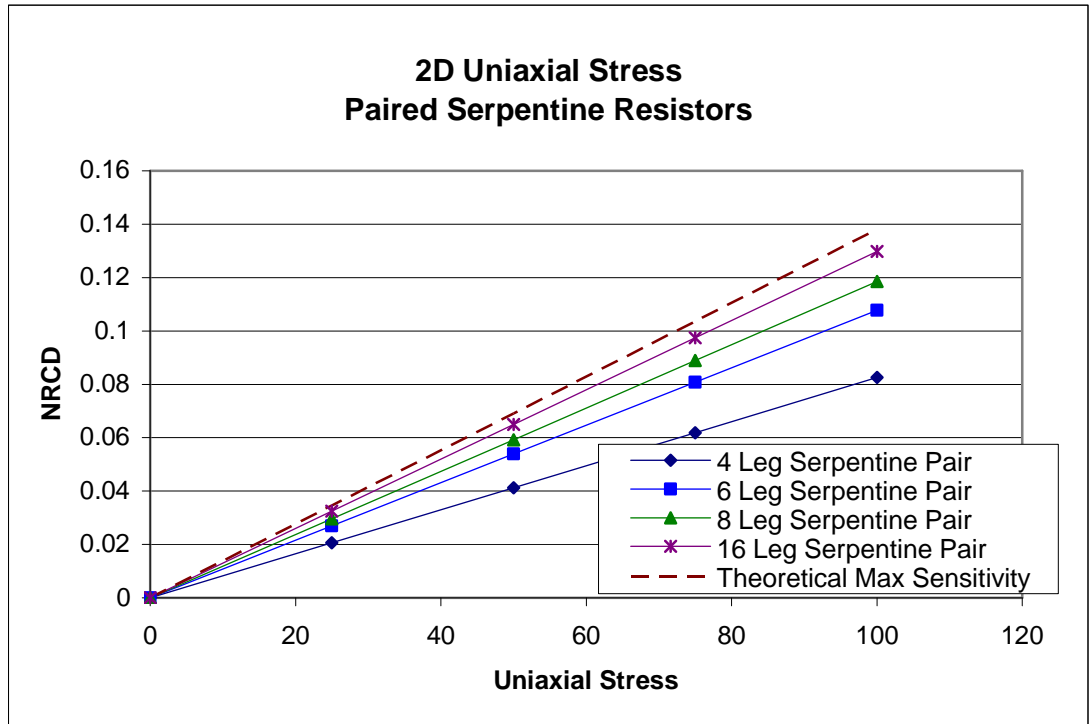


Figure 19. Sensitivity of serpentine resistor pairs with variable number of legs.

As the number of legs increases in the meshes shown in Figure 18, NRC D of the serpentine resistor increases. This is probably a result of the decreasing importance of the fixed width leg interconnects. For larger leg sizes it can be seen that the interconnect regions contribute resistance to the sensor, but yield only transverse (lower than longitudinal) strain sensitivity. As the legs become narrower, the fixed width interconnects contribute less resistance to the unstressed structure, and the sensor approaches the theoretical device sensitivity. It should be noted that the unstressed resistances for each sensor configuration vary greatly due to the increased length and decreased width. The 16-leg sensor has an unstressed resistance of $1.668 \text{ M}\Omega$ as compared to a nominal resistance of $122 \text{ k}\Omega$ for the 4 leg sensor.

These results indicates that the 2D FEA analysis is giving results consistent with theoretical values and confirms that for the analyses we have developed here, the VDP geometry under identical conditions to the serpentine resistor geometry yields an NRCD value more than 3 times higher: 4.35 GPa^{-1} compared to 1.38 GPa^{-1} . With these results established for the 2D case, the full 3D model with non-uniform stress will be subsequently developed.

Summary of Results

A summary of all the relevant results for the 2D analyses of the VDP and serpentine resistors are presented in Table 3. MATLAB results are not presented for the serpentine resistor, as the geometry was prohibitive to implement in the specialized code. It can be seen FEA values closely match the theoretical values for both sensor types.

Table 3. Summary of 2D analysis results

Sensor	Value	Sensitivity	Units
VDP	Theoretical Sensitivity	4.401	GPa^{-1}
	Uniaxial Stress Sensitivity – MATLAB	4.358	GPa^{-1}
	Uniaxial Stress Sensitivity – ANSYS 2D	4.351	GPa^{-1}
Serpentine	Theoretical Sensitivity	1.381	GPa^{-1}
	Uniaxial Stress Sensitivity – ANSYS 2D – 4 legs	0.825	GPa^{-1}
	Uniaxial Stress Sensitivity – ANSYS 2D – 6 legs	1.076	GPa^{-1}
	Uniaxial Stress Sensitivity – ANSYS 2D – 8 legs	1.185	GPa^{-1}
	Uniaxial Stress Sensitivity – ANSYS 2D – 16 legs	1.298	GPa^{-1}

3D FINITE ELEMENT ANALYSIS

3D ANSYS Model

To model the stresses that will be developed in a working piezoresistive pressure sensing device, a full 3D model was created in ANSYS. The model was created with tetrahedral elements of type SOLID187, the geometry of which is shown in Figure 20. The element supports full anisotropic elasticity, which is specified via the TBDATA command.

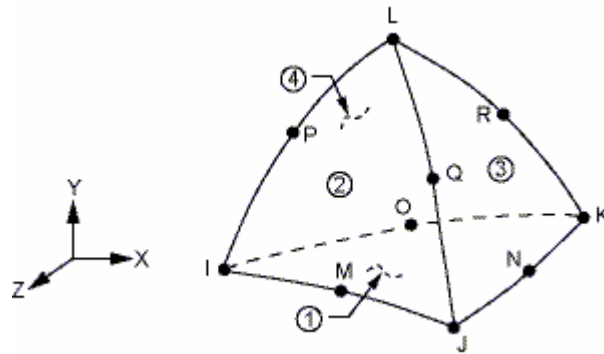


Figure 20. SOLID 187 element. a 10 node element that supports anisotropic elasticity.

The geometry of the diaphragm before and after solution is shown in Figure 21. The model was simplified by employing a symmetry plane at the center of the diaphragm. The model represents the geometry of a silicon pressure sensor. To model the effect of the diaphragm being tested as part of a larger silicon wafer, or as bonded to a substrate, the bottom surface of the diaphragm, as well as all the sides have all degrees of freedom fixed. The top surface has a normal surface pressure applied, representing the gage pressure applied across the diaphragm surface. The geometric parameters and material

properties given in Table 4 are used in this and all subsequent 3D analyses, unless otherwise noted.

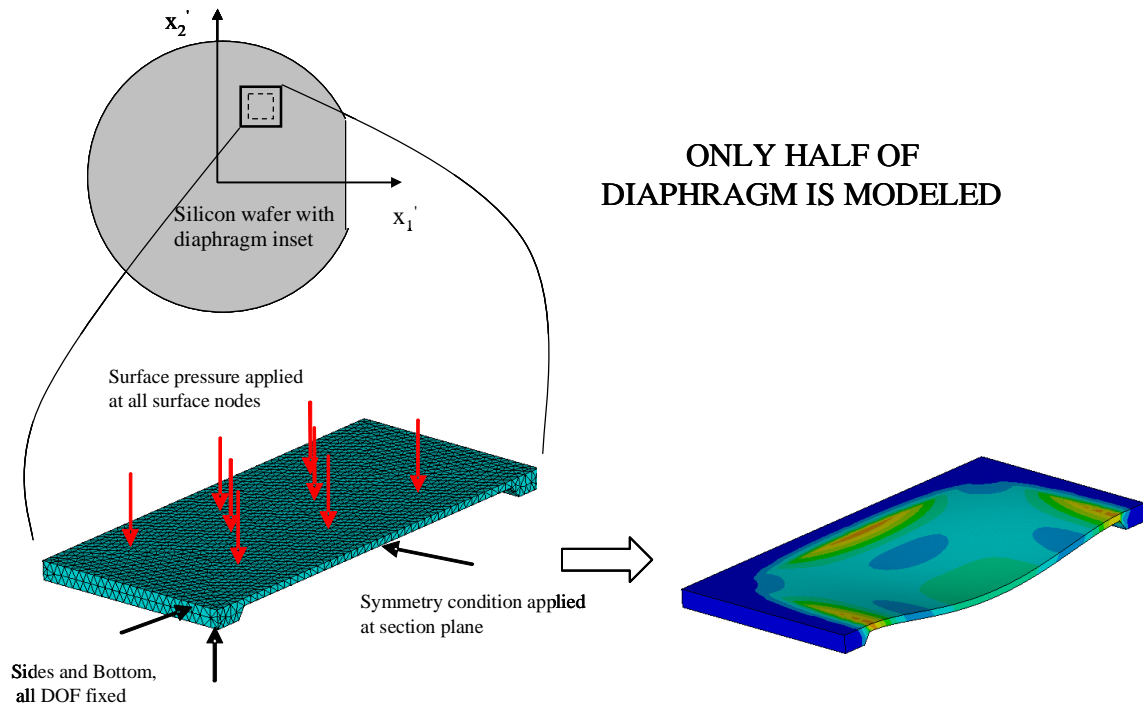


Figure 21. 3D Diaphragm model geometry. a) meshed ANSYS model, showing locations of applied boundary conditions, and b) displacement solution (exaggerated) with color indicating stress.

Table 4. Geometric parameters and material properties.

Geometric Parameter	Value	Units	Material Property	Value	Unit
Diaphragm Thickness	200	μm	Elastic Moduli		
Diaphragm Size	10 x 10	mm	E_{11}	165.7	GPa
Total Wafer Thickness	525	μm	E_{12}	63.9	GPa
Base support Width	1000	μm	E_{44}	79.6	GPa
			Resistivity of p-type Si	7.8	$\Omega\text{-cm}$
			Piezoresistive Coefficients		
VDP depth	20	μm	π_{11}	6.6	10^{-11} Pa
VDP Size	125x125	μm	π_{12}	-1.1	10^{-11} Pa
Applied Voltage	5.0	V	π_{44}	138.1	10^{-11} Pa

Effect of Stress Stiffening in Diaphragm

The diaphragm model was solved with and without stress stiffening enabled (NLGEOM command) to validate the assumption that the small diaphragm is in the small displacement regime. When solved with 10 solution substeps, and at a diaphragm pressure of 100kPa the maximum component stress in the diaphragm was found to be 68.5 MPa near diaphragm edge. The maximum stress value without incorporating stress stiffening was 68.0 MPa. The error in stress is therefore 0.7%, a result which justifies the considerable savings in computational time by neglecting stress stiffening effects. The corresponding maximum nodal displacements (at diaphragm center) were 13.093 μm and 13.078 μm , an error of 0.1%. The displacement at diaphragm center of 13 μm is approximately 6% of the diaphragm thickness of 200 μm .

Submodeling

After determining the displacement solution of the 3D diaphragm model, a submodeling technique was introduced in modeling in the VDP solution. This was done

for several reasons: 1) Efficiency; analysis of multiple VDP geometries and positions can be performed for a given pressure without having to resolve the diaphragm displacement solution 2) Nodal count, the educational license of ANSYS permits no more than 32000 nodes, which is easily exceeded with a fine 3D mesh. 3) Post processing is simplified with only submodeled elements to deal with. The submodeling process works as follows and is depicted below in Figure 22.

1. Solve adequately fine diaphragm mesh to determine displacement solution, save model and results to database.
2. Start new analysis, build submodeled region. The global coordinates of the submodel geometry must correspond to the global coordinates of the equivalent region in the diaphragm model.
3. Select boundary nodes on submodeled region. These nodes will have their displacement DOF's fixed according to the displacement solution of diaphragm. Export list of selected nodes and nodal positions to a text file
4. Open diaphragm model, use **CBDOF** command to import nodal position list and to export text file containing interpolated displacement solution for each imported nodal position.
5. Open submodel analysis and import list of DOF commands

The restrictions on this method are that the original mesh is sufficiently fine such that the interpolation procedure of the submodel is not subject to significant errors, and that the area of analysis within the submodel is sufficiently far from the submodel boundary

that St. Venant's principle applies. Here the characteristic length is the nodal spacing at the submodel boundary.

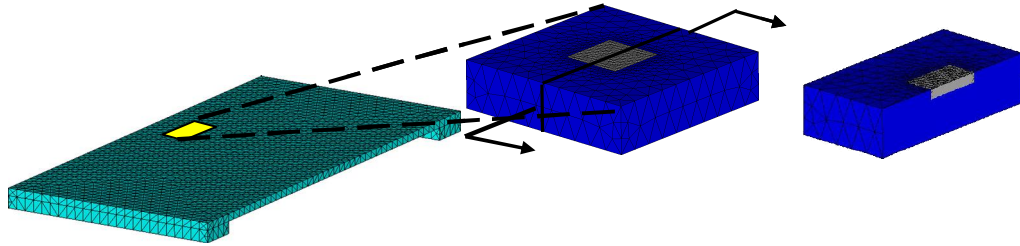


Figure 22. Submodeled analysis region and cross-section showing sensor area

The submodel region is shown in Figure 22. The VDP region is meshed with SOLID227 elements, and the surrounding submodel region is modeled with SOLID187 elements. Both of these elements have the same geometry (see Figure 20). The SOLID227 element is a coupled-field element which supports piezoresistivity when used with KEYOPT=101. The 36 piezoresistive components are specified using TBDATA. For silicon there are only 3 independent piezoresistive coefficients, given in Table 4.

The solution procedure for the submodel is as follows. First, the VDP size, depth, angle and x and y position on the diaphragm are determined. The submodel is then created in a coordinate system centered at the (x,y) position of the VDP. The geometry is meshed and has boundary DOF's specified as described above. The voltage DOF's are specified in either a 0° or 90° orientation. (Both orientations are independently built and solved for each run of the model), and the model is solved. For each of the 0° and 90° orientations the results are postprocessed. First, the voltage at the opposite corner nodes

can be read directly from the solution output. The difference between these two values is stored as V_{out} . To determine current through the VDP, a cutting surface is established through the VDP geometry, normal to the direction of current flow, and the conduction current result vectors are projected onto the surface. The mapped results are then integrated over the cross sectional surface. The resulting value is the total current flowing through the VDP. Dividing the output voltage by the integrated current value yields the “Resistance” of the VDP for either a 0° or 90° orientation. Taking the stressed resistances for both 0° and 90° orientations, as well as the unstressed resistance, the NRCD can then be calculated using Eqn. (19).

Pressure Sensitivity of VDP

To determine the sensitivity of the VDP structure as part of a pressure sensing diaphragm, the 3D ANSYS model was solved first for an unstressed diaphragm and then for various diaphragm pressures. It should be noted that the stress that the VDP senses for a given diaphragm pressure is entirely dependent on the diaphragm geometry. Therefore the following results are quantitatively true only for specific diaphragm and VDP dimensions. However, the qualitative behavior will not change for simple changes in dimension.

The results are given as a function of NRCD in Figure 23. The average stress in the figure is calculated differently for the 3D model then for either of the 2D models. For the 2D uniaxial stress, σ_{yy} is assigned and σ_{xx} is zero. In the 2D biaxial stress case σ_{yy} and σ_{xx} are assigned, with $\sigma_{xx} = \nu\sigma_{yy}$ where ν is close, but not exactly equal to Poisson’s ratio for the anisotropic material. For both 2D cases the average stress is the stress everywhere

throughout the sensor. To calculate a comparable stress for the 3D VDP, the x and y element stresses are summed for every element in the 3D VDP region, and then divided by the number of elements in that region.

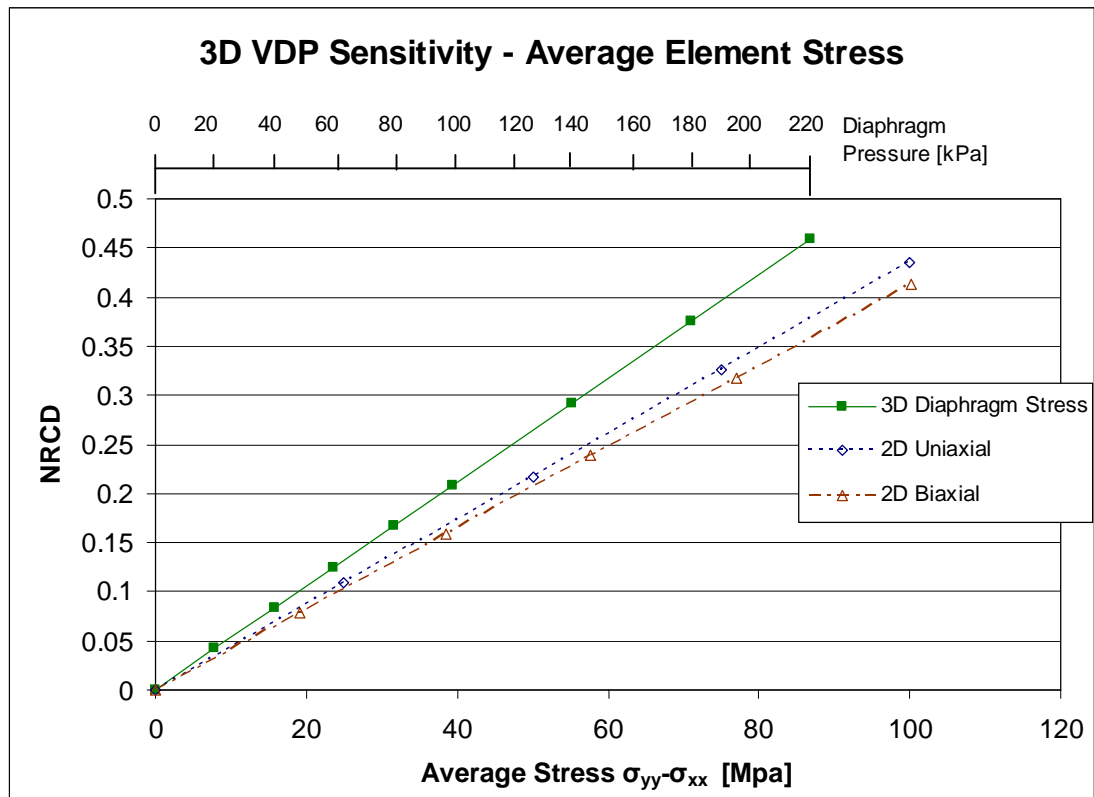


Figure 23. Sensitivity of 3D VDP as compared to 2D analyses. Diaphragm pressure required to generate stress.

As can be inferred from figure the diaphragm based sensor has higher sensitivity per unit of average stress than the 2D sensors. This effect is most likely a result of the averaging method used. For each of the diaphragm data points in the figure, the maximum measured element stress in the VDP is 62% greater than the average element stress. Because of the large stress variation in the element it is unclear whether the

“average” element stress truly captures the average importance of that stress. An element experiencing increased stress in a certain region of the 3D VDP volume does not necessarily increase the VDP current by the same amount as would an element of increased stress elsewhere in the volume. To get a true basis of comparison, a weighted average of the element stresses would have to be taken, where the weighting function captured the importance of the element position to the NRCD of the sensor. This has not been attempted, for our present purposes it is sufficient to compare the sensitivity of the 3D sensor to those 2D sensors that have already been analyzed. It is seen that the 3D sensitivity is comparable to that of the 2D sensors, acknowledging that in moving to the more complex 3D stress state we have lost the analytical stress basis for comparing the two. As a final check, the stress states (calculated by averaging) for the line labeled *3D diaphragm stressing* the above figure were applied uniformly to a 3D model of the VDP structure (not submodeled). When the sensitivity was calculated, it was found to match the 2D uniaxial and biaxial stress states exactly. This confirms that the averaging method is responsible for the discrepancy between the 2D and 3D models in the figure. And the true average stress that the VDP is sensing is higher than that shown in Figure 23.

The goal of the following analyses is to optimize the values of the geometric and positional parameters of the VDP, to obtain the highest possible sensitivity. Model values are the same as those given in Table 4, unless otherwise noted. In all of the following analyses the pressure applied to the diaphragm is 100 kPa, as this will be the maximum test pressure that prototypes will eventually be subjected to.

Positional Optimization

Using the 3D ANSYS model, a variety of geometric parameters were varied to determine those values that yield the highest sensitivity device. The transverse sensitivity is the sensitivity to position in the x-dir, as indicated in Figure 24.

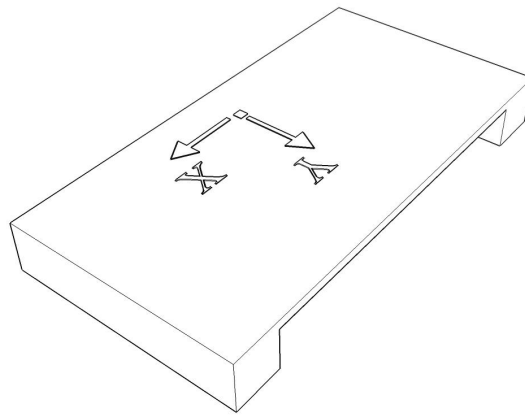


Figure 24. Coordinate system for position analysis. Origin is positioned over edge of diaphragm.

The longitudinal dependence is sensitivity dependence on VDP position in y-direction. Both positional sensitivities are given as a percent of distance from origin to diaphragm corner or center, respectively. The stress distribution for a typical solution is given in Figure 25. Note that deflection is exaggerated by a factor of 30 for visualization.

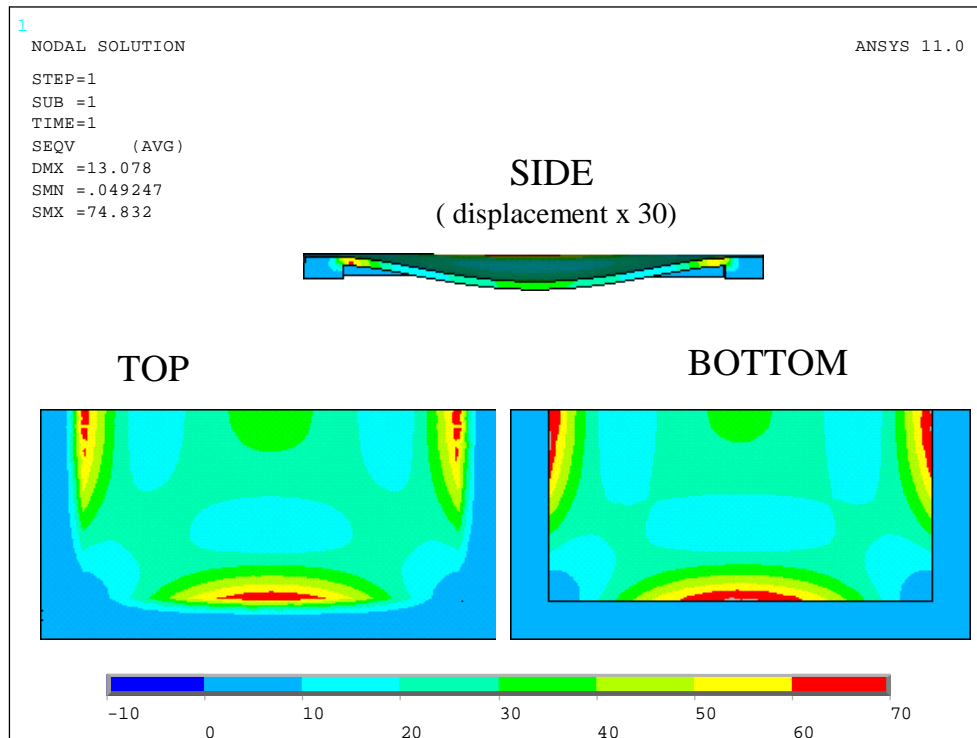


Figure 25. Von Mises stress distribution in half diaphragm model at 100kPa.

Longitudinal Position Dependence

The longitudinal dependence analysis was examined first, a plot of sensitivity as a function of y-position is presented in Figure 26. The results show a strong peak in sensitivity at 2.4% offset towards center. For the 1 cm x 1cm diaphragm modeled here, 2.4% corresponds to $\sim 120 \mu\text{m}$. This position corresponds with the location of maximum stress as seen in Figure 25.

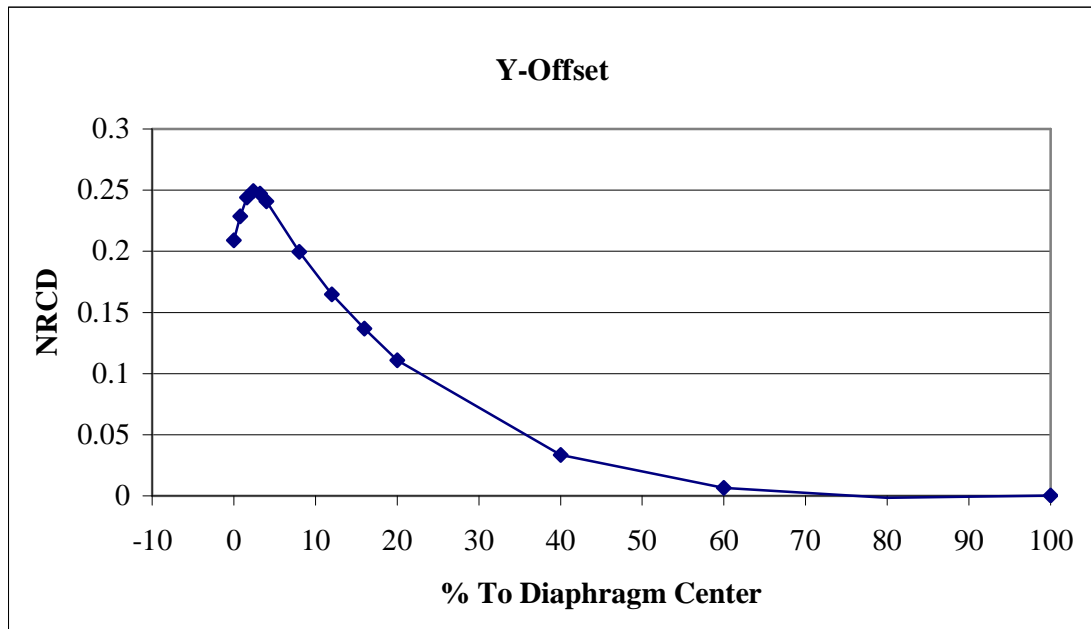


Figure 26. Longitudinal position analysis. The sensitivity of the VDP on a square diaphragm is strongly dependent on position, with a peak at 2.4% offset towards center.

This 2.4% offset was carried forward into additional analyses, the goal being to develop gradual isolate the most sensitive VDP position and geometry.

Transverse Position Dependence

The results of the transverse (x-direction) position dependence are provided in Figure 27. The results are again given as a percent offset from edge center to corner. Not surprisingly, from a visual inspection of the stress profile, the maximum sensitivity is found along the symmetry plane of the diaphragm. Here however the sensor is relatively more tolerant to positional error in the x-direction than in the y-direction. With a VDP

sensor size of $125 \times 125 \mu\text{m}$, even at a distance of 10 sensor widths, the sensitivity goes down by only 10%.

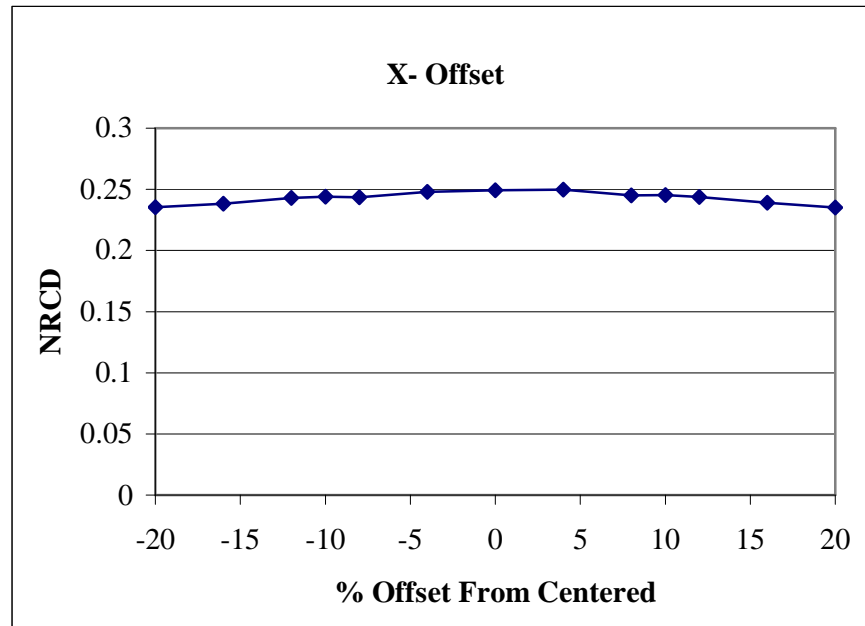


Figure 27. Transverse sensitivity analysis. Highest sensitivity is for centered VDP.

For the remaining sensitivity analyses, a 0% offset is used and the $125\mu\text{m}$ offset in the longitudinal direction is maintained.

Angular Alignment Dependence

The effect of misalignment of the VDP sensor with respect to the diaphragm geometry is also considered. Models were solved and post processed for VDP angles of -30 to +30 degrees relative to the diaphragm axes. These results are consistent with the results for p-type silicon from the finite difference analysis, as in Figure 8. During the wafer processing steps required to produce this sensor, it is possible for misalignment to

occur between the front and back masks. However, 5° alignment accuracy is relatively easy to attain, and thus the sensitivity results for this analysis indicate that special controls need not be employed to obtain a sensitive device.

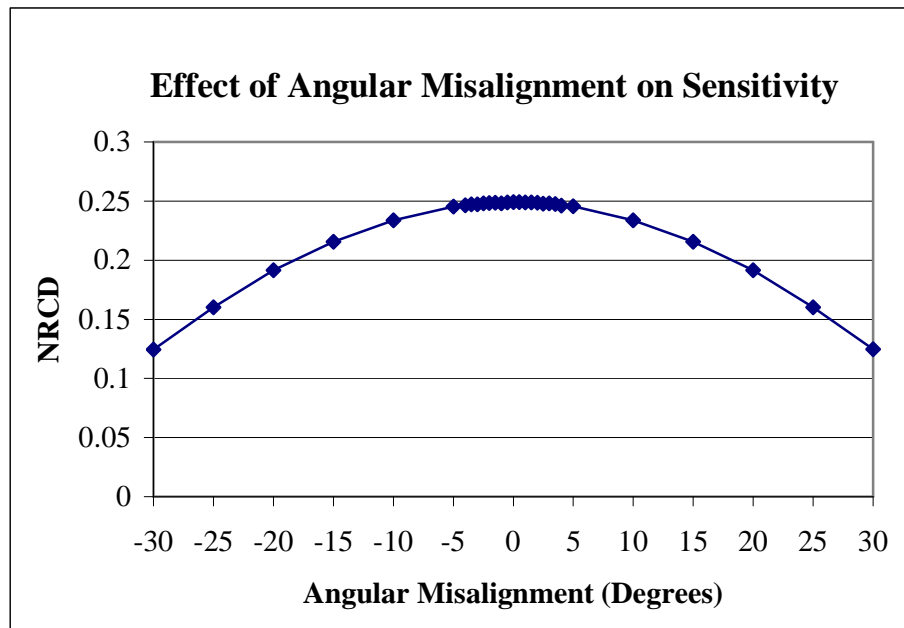


Figure 28. Angular sensitivity analysis. The VDP is tolerant of angular misalignment of up to 5 degrees, beyond which it drops significantly.

Geometric Optimization

Aside from position of the VDP sensor on the diaphragm, it is necessary to select the VDP geometry such as to yield the highest attainable sensitivity. The only geometry parameters that are investigated here are the depth and size of the VDP. More complicated geometries will be investigated later.

Size Dependence

The size dependence of the VDP sensitivity was considered for a range of 50-200 μm . Larger sizes were not considered because they begin to overlap the diaphragm boundary, where the stress profile changes considerably. Sizes below 50 μm were not considered as the required number of nodes began to exceed the software limits. Regardless, it is clear from Figure 29 that smaller sensors are slightly more sensitive than larger sensors, likely as a result of being located more completely inside the peak stress region.

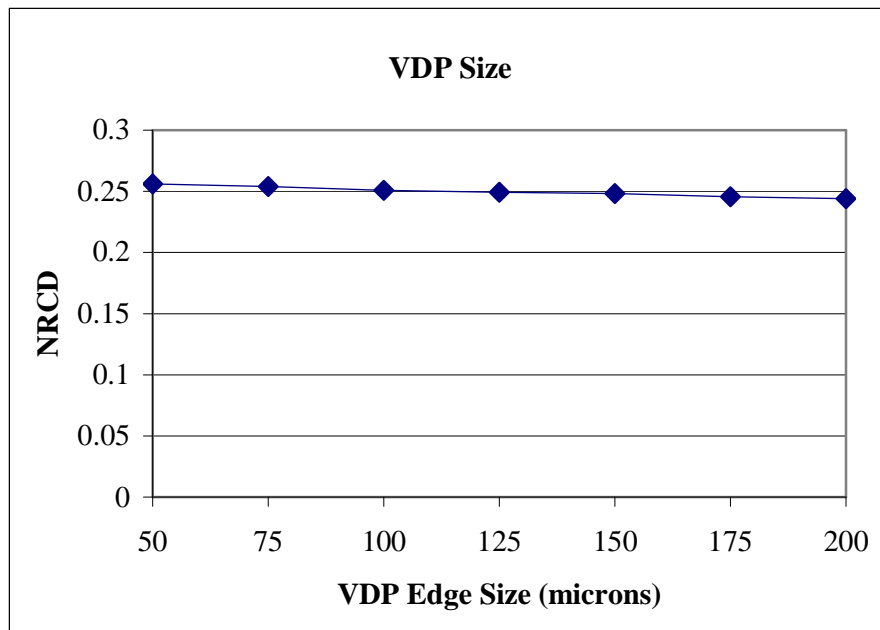


Figure 29. VDP size sensitivity analysis. The VDP is not strongly dependent on size.

Depth Dependence

The final sensitivity analysis was for the depth of the VDP. The results are presented in Figure 30. Again, there is a slight linear dependence of sensitivity on depth. A thinner VDP exhibits higher sensitivity, likely as a result of existing more completely in a high

stress area (i.e. not averaging in lower stresses). It should also be noted that for varying VDP thicknesses, the unstressed resistance varies as given in Eqn. (10). The analytical result is confirmed in this analysis. Halving the VDP thickness doubles its unstressed resistance, and therefore in integrating the sensor into a control circuit, the thickness may be tuned not only to increase sensitivity, but also to keep the stressed or unstressed resistances within a desired range.

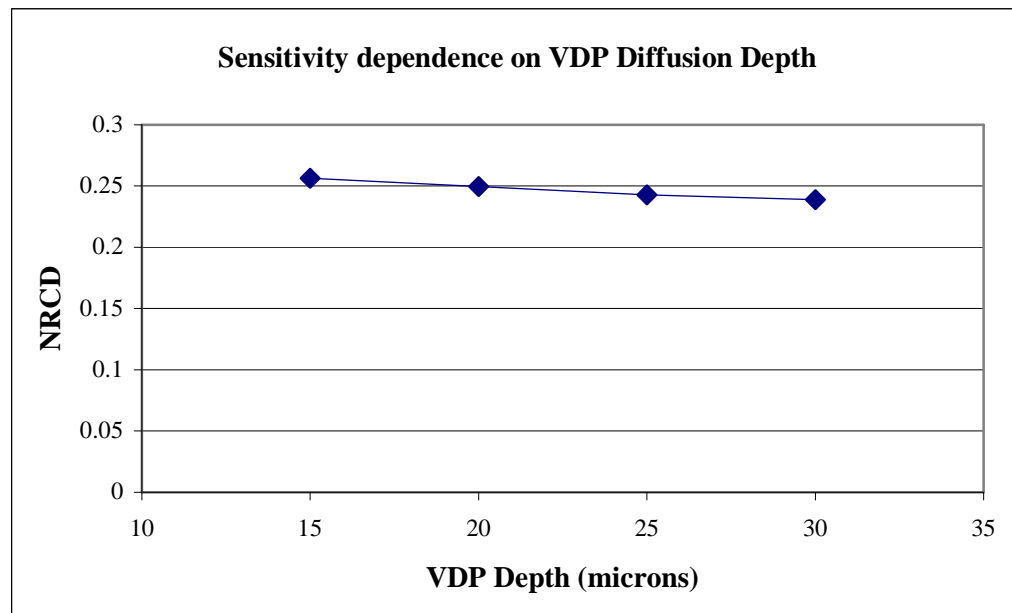


Figure 30. VDP depth sensitivity. A shallower VDP has higher sensitivity.

Pad Size Dependence

Electrodes at the top surface of the VDP are required as electrical connection points. The size of these electrodes creates a departure from the models that have been thus far analyzed. The change in resistance due to pad size is estimated by van der Pauw [4]. In that analysis, the electrode widths were radial lengths on a circular VDP structure. It was

determined that the change in resistance due to pad size effects was of order of the square of the ratio of the electrode size to the edge length. For a pad size of 10% of the VDP edge length, this corresponds to a change in resistance of approximately 1-2 %. This was confirmed in ANSYS analyses, for pad sizes of ~12 microns. It is desirable, however, that the pad size be made as small as feasible to obtain optimal results.

Comparison to Analytical Results

The displacement solution of the 3D diaphragm was also obtained analytically. There are a number of approximate solutions for the rectangular plate with all edges built in. These results give only values of engineering interest such as maximum bending stress, moment, and deflection. Empirical values for these values are given by Timoshenko, Hencky, and Meleshko, and an excellent investigation of the general problem is given by Meleshko [16]. These approximations require two conditions that do not apply for the silicon diaphragm: the results are accurate only for isotropically elastic material, and they assume a built in edge. Silicon is orthotropic, and the diaphragm geometry we consider allows some strain in the tapered region between the diaphragm and the base. Nonetheless, these calculations were performed using Mathcad. They are presented in Appendix D. Additionally, the full diaphragm displacement solution was obtained using Levy's method as implemented by Timoshenko [17]. These calculations are presented in said Appendix. For similar diaphragm geometry and approximating the modulus of silicon as linear, the results were calculated are provided in Table 5.

The approximate results for peak stress in the diaphragm yields a value of 77 Mpa, which is within 5% ANSYS FEA result as in Figure 25. There is a larger discrepancy in

the maximum deflection of the diaphragm center. ANSYS yields a value 25% lower than the analytical solution, 13.1 micron displacement compared to 17.3 microns for 100 kPa diaphragm pressure. This result is due to the anisotropic elasticity of silicon. The analytical results confirms the qualitative stress distribution over whole diaphragm area and the maximum stress values in the diaphragm, which are those of interest in the sensor design.

Table 5. Analytical stressed diaphragm results

Method	Peak Equivalent Stress	Diaphragm Displacement
Timoshenko	77.0 MPa	17.2 micron
Meleshko	77.1 Mpa	17.4 micron
Hencky	77.0 MPa	17.3 micron
Series Solution	62 MPa	17.0 micron
FEA Ansys	74 Mpa	13.1 micron

A Composite VDP Structure

The Picture Frame

A composite VDP structure was modeled in an effort to increase the sensitivity of the device. Motorola has used such geometry in piezoresistive pressure sensor, with a different electrode configuration than used here. Motorola's picture frame is based on the terminal layout of the FTT structure, which they refer to as the "Xducer". Here the VDP terminal layout is instead used. A pressure sensitivity analysis was performed with what found to be the peak stress location in the previous chapter. The picture frame geometry is show in Figure 31. Supply and output voltages were applied to the same corners as in the VDP geometry, and simulations were run for both 0° and 90° orientations. As shown

in Figure 32, the Picture Frame has lower sensitivity than the regular VDP at the peak stress location.

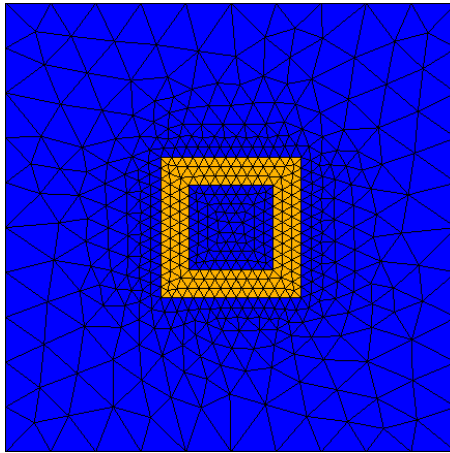


Figure 31. The submodeled picture frame geometry.

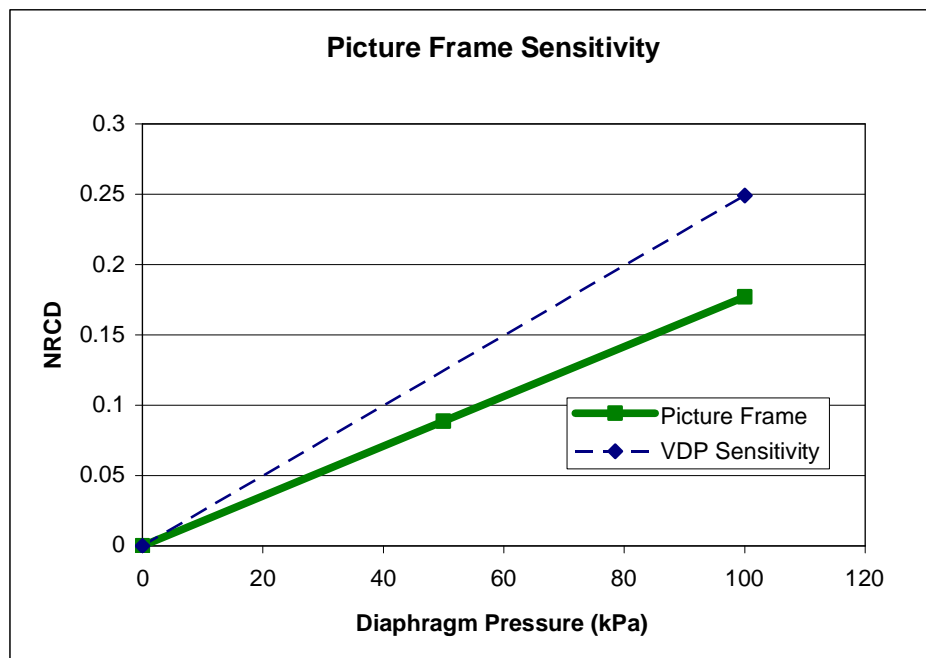


Figure 32. Comparison of 'Picture Frame' to VDP sensitivity.

The above results are not surprising. Although the above sensor would maintain the temperature compensating properties of the VDP, the distributed nature of the sensor has decreased. The sensitivity of the VDP structure arises from the total area that is able to contribute to strain sensing, relative to the amount of current that is flowing through the sensor. The VDP structure has the most contributing sensing area per unit resistance of any such sensor. The 'picture frame' sensor analyzed here, has higher resistance per unit area, and less strain sensing area, resulting in lower sensitivity. No other structures have been proposed that would yield greater sensitivity given the same area.

Summary of Results

The sensitivity values for the 3D ANSYS VDP analysis cannot be compared directly to those for the 2D VDP analysis as in Table 3, because the stress is nonuniform through the sensor in the 3D analysis as described earlier. Nonetheless, a measure of the sensitivity of the device as it relates to the specific diaphragm geometry examined herein can be provided. Taking a value of the NRCD as 0.25, even though higher values may be obtainable, the normalized voltage output is calculated per unit test pressure. For an NRCD of 0.25 on a 1.0 cm square diaphragm of thickness 0.2 mm, the unstressed output voltage is 8.2 mV/V. The output voltage increases beyond this value 1.07 mV/V/100kPa in the 0° orientation. The output voltage decreases from the unstressed value by 0.95 mV/V/100kPa in the 90° orientation. The voltage difference between these two measurements is therefore 2 mV/V/100 kPa or 20 μ V/V/kPa.

The 3D diaphragm analysis indicates that the theoretical and numerical results for the NRCD of the sensor are in good agreement. The VDP structure has been shown to have a NRCD three times greater than that of a conventional piezoresistor, while requiring only a single sensor to enable a temperature compensated measurement.

CONCLUSIONS

In the work presented here the VDP structure was modeled on several different levels. The sensor was modeled and the behavior solved using a 2D finite difference approximation. Then the device was modeled in ANSYS, beginning with a 2D solution. The FEA analysis was then extended into 3D under contrived stress states, and finally the VDP geometry was modeled in 3D FEA using the submodeling technique. Here, the stress states were those from a square diaphragm micromachined from p-type Si.

Starting from established theoretical work on stress measuring properties of the sensor, the sensor structure was first modeled with MATLAB by solving the partial differential equations with custom built finite difference routines. In that analysis, the small strain effects were neglected, but excellent agreement between theoretical and numerical data was obtained.

In order to generate more complex stress states, and to analyze a greater number of models with more complex geometries, the 2D model was moved into ANSYS, and the VDP was again analyzed, in addition to the conventional piezoresistive device. Again, excellent agreement was obtained between theoretical and finite element models.

The model was then analyzed in 3D to establish convergence of the model results. The stress states of a square diaphragm were determined by solving the square diaphragm under pressure and submodeling the VDP sensor into the stress field of the solution. This method allowed for optimization of VDP geometry and position. The optimization procedure provides a guide for the manufacturing of the test sensors.

Furthermore, the VDP shows promise in MEMS pressure sensing devices that demand ever smaller transducer sizes. The sensor's simple geometry and inherent temperature compensation characteristics are expected to be valuable in finding application for this sensor in future transducer designs.

The VDP structure has a "resistance" independent of its size, and dependent only on thickness. This enables significant miniaturization of the sensor geometry, while maintaining the ability to have a nominal resistance that is suitable for integration with the rest of the signal conditioning circuit.

Experimental Methods (Ongoing Work)

The diaphragms and sensors modeled in the previous chapter were designed and photolithographic masks were fabricated. The sensors will be manufactured using standard fabrication procedures as currently modeled and the test results will be compared to the above theoretical results. The layout of sensors and diaphragms for the prototype test wafer is shown in Figure 33. The test wafer consists of diaphragms of three different sizes:

10 mm x 10 mm (12)

5 mm x 5 mm (6)

20 mm x 20 mm (1)

Each diaphragm has a different VDP geometry with regards to position, size, or alignment. Some of the diaphragms incorporate a serpentine piezoresistor for experimental verification of the sensitivity increase of the VDP over the serpentine

piezoresistor. Additionally, a test strip is incorporated for measurement of the piezoresistive coefficients of the material.

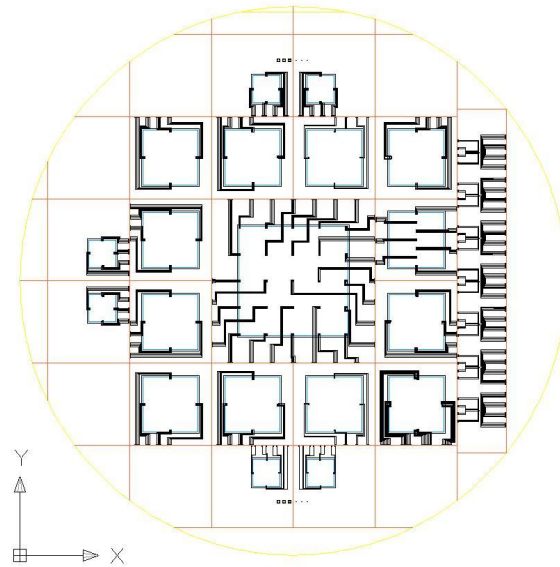


Figure 33. Circuit and mask layout for characterization of pressure sensors.

Additionally, the VDP needs to be characterized for noise sources and a noise floor needs to be established to obtain the obtainable pressure resolution in a diaphragm based pressure sensor. Shot noise, thermal noise, and $1/f$ noise should all be characterized to determine the real performance of this device in application. Preliminary calculations indicate that the thermal noise at operating temperature should be on the order of 100 nV at 1 kHz, and at lower measurement frequency should be reducible to ~ 10 nV. The VDP sensor on the diaphragm as proposed should therefore be able to attain pressure resolution on the order of 10 Pa. This is a crude estimate however, and a great deal of measurement and amplification circuitry will need to be designed before this sensor finds application.

REFERENCES CITED

1. W. G. Pfann, R.N.T., *Semiconducting Stress Transducers Utilizing the Transverse and Shear Piezoresistance Effects*. Journal of Applied Physics, 1961. **32**(10): p. 2008-2019.
2. Jahsman, W.E., *Biaxial Gage Factor for Piezoresistive Strain Gages*. Experimental Mechanics, 1979. **19**(11): p. 411-415.
3. D. A. Bittle, J.C.S., R.E. Beaty, R. C. Jaeger, R.W. Johnson, *Piezoresistive Stress Sensors for Structural Analysis of Electronic Packages*. Journal of Electronic Packaging, 1991. **113**: p. 203-214.
4. van der Pauw, L.J., *A Method of Measuring Specific Resistivity and Hall Effect of Discs of Arbitrary Shape*. Philips Research Reports, 1958. **13**: p. 1-9.
5. van der Pauw, L.J., *Determination of Resistivity Tensor and Hall Tensor of Anisotropic Conductors*. Philips Research Reports, 1961. **16**: p. 187-195.
6. Mian, A.K.M., J.C. Suhling, and R.C. Jaeger. *Sensitivity of (100) Silicon VDP Sensors to Uniaxial and Hydrostatic Loads*. in *Proceedings of SECTAM-XX*. 2000. Callaway Gardens, Pine Mountain, GA.
7. Mian, A., J.C. Suhling, and Richard C. Jaeger, *The van der Pauw Stress Sensor*. IEEE Sensors Journal, 2006. **6**(2): p. 340-356.
8. Schmidt, R., *Universal intelligent pressure transducer for automotive applications*. Elektronik Praxis, 2000. **No 20**: p. 62-64.
9. Schuster, J.P. *Automotive Silicon Based Pressure Transducers for Fluid Power Applications*. in *Proceeding of the National Conference on Fluid Power, Annual Meeting*. 1986.
10. S. Marco, J.S., O. Ruiz, J.R. Morante, J. Esteve, *High Performance piezoresistive pressure sensors for biomedical applications using very thin structured membranes*. Meas. Sci. Technol., 1996. **7**: p. 1195-1203.
11. Smith, C.S., *Piezoresistance Effect in Germanium and Silicon*. Physical review, 1954. **94**: p. 42-49.
12. P.J. French, A.G.R.e., *Polycrystalline Silicon as a Strain Gauge Material*. J. Phys. E: Sci. Instrum, 1986. **19**: p. 1055-1058.
13. Wortman, J.J. and R.A. Evans, *Young's Modulus, Shear Modulus and Poisson's Ratio in Silicon and Germanium*. Journal of Applied Physics, 1965. **36**(1): p. 153-156.

14. Mitchell, A.R. and D.F. Griffiths, *The finite difference method in partial differential equations*. 1980, Chichester [Eng.] ; New York: Wiley. xii, 272 p.
15. *ANSYS Multiphysics 10.0 Educational Version*. 2005, Ansys, Inc.
16. Meleshko, V.V., *Bending of an Elastic Rectangular Clamped Plate: Exact Versus 'Engineering' Solutions*. Journal of Elasticity, 1997. **48**: p. 1-50.
17. Timoshenko, S., *Theory of Plates and Shells*. 2 ed. Vol. 1. 1959, New York: McGraw-Hill 568.

APPENDICES

APPENDIX A

MATLAB ROUTINES

VDPBOTH_PSENS.M

```

% CALL STACK
%
%
% *** vdpboth_psens.m ***
%   |
%   |_ vdpsim_psens.m
%       |_ vdpsimDRIVER.m
%           | (material props)
%           |_ RV_ROT.m
%           |_ vdpsim.m
%
%   |_ vdptheory_psens.m
%       |_ vdptheory.m
%           | (material props)
%           |_ FourthRank2D.m
%
%
hold off
[a,b]=vdptheory(1,'n',-1,-1);
set(gca,'LineStyle',':');
hold on
set(gca,'LineWidth',2)
[a,b]=vdptheory(1,'p',-1,-1);
title({'Normalized Resistance Change Difference';'Angular (\phi)
dependence of Sensor on Diaphragm';
'n-Type and p-Type Silicon'});
legend('n-Type','p-Type')
H=gcf;
set(H,'color',[1 1 1]);
hold off

nu=0.27;
t=0.002;
R=0.05;

if ~exist('press_theory')
vdptheory_psens
sigrr_theory=(-3.*press_theory)./(8*t^2)*(((1+nu)*R^2-(3+nu)*R^2));
sigtt_theory=(-3.*press_theory)./(8*t^2)*((1+nu)*R^2-(1+3*nu)*R^2);
press_theory=(sigrr_theory-sigtt_theory)./10^7;%dyne/cm^2
end
if ~exist('press_sim')
vdpsim_psens
sigrr_sim=(-3.*press_sim)./(8*t^2)*(((1+nu)*R^2-(3+nu)*R^2));
sigtt_sim=(-3.*press_sim)./(8*t^2)*((1+nu)*R^2-(1+3*nu)*R^2);
press_sim=(sigrr_sim-sigtt_sim)./10^7;
end

% press_theory=(-3.*press_theory)./(8*t^2)*(((1+nu)*R^2-(3+nu)*R^2));
%dyne/cm^2

```

```

% press_sim=(-3.*press_sim)./(8*t^2))*(((1+nu)*R^2-(3+nu)*R^2));
% % Convert pressure to MPa radial stress
% press_theory=press_theory./10^7
% press_sim=press_sim./10^7

%plot(press_sim,pNRCsim(:,1),':xr',press_sim,pNRCsim(:,2),':xb')
figure
plot(press_theory,pNRCtheory(:,1),'-
or',press_sim,pNRCsim(:,1),':xr',press_theory,pNRCtheory(:,2),'-
sb',press_sim,pNRCsim(:,2),':+b')
title({'p-Type silicon';
'\phi = 0\circ'});
legend('\Delta R^{\sigma}_{0\circ} -
Theoretical','\Delta R^{\sigma}_{0\circ} - Simulated', ...
'\Delta R^{\sigma}_{90\circ} - Theoretical',
'\Delta R^{\sigma}_{90\circ} - Simulated')
axis([0 70 -0.2 0.2]);
xlabel('Stress Difference \sigma_{rr}-\sigma_{\theta\theta} (MPa)');
ylabel('Normalized Resistance Change');
H=gcf;
set(H,'color',[1 1 1]);
    hold off

figure
%plot(press_sim,nNRCsim(:,1),':xr',press_sim,nNRCsim(:,2),':xb')
hold on
plot(press_theory,nNRCtheory(:,1),'-
or',press_sim,nNRCsim(:,1),':xr',press_theory,nNRCtheory(:,2),'-
sb',press_sim,nNRCsim(:,2),':+b')
title({'n-Type silicon';
'\phi = 0\circ'});
legend('\Delta R^{\sigma}_{0\circ} -
Theoretical','\Delta R^{\sigma}_{0\circ} - Simulated', ...
'\Delta R^{\sigma}_{90\circ} - Theoretical',
'\Delta R^{\sigma}_{90\circ} - Simulated')
axis([0 70 -0.2 0.2]);
xlabel('Stress Difference \sigma_{rr}-\sigma_{\theta\theta} (MPa)')
ylabel('Normalized Resistance Change')
box on
    H=gcf;
set(H,'color',[1 1 1]);
hold off

```

VDPSIMDRIVER.M

```

%%%%%%%%%%%%%%%%%%%%%%%%%%%%%%%%%%%%%%%%%%%%%%%%%%%%%%%%%%%%%%%%%%%%%%%%
%%%%%%%%%%%%%%%%%%%%%%%%%%%%%%%%%%%%%%%%%%%%%%%%%%%%%%%%%%%%%%%%%%%%%%%%
% CALL STACK
%
%
% vdpboth_psens.m
%   |
%   |_ vdpsim_psens.m
%       |_ **** vdpsimDRIVER.m ****
%           | (material props)
%           |_ RV_ROT.m
%           |_ vdpsim.m
%
%   |_ vdptheory_psens.m
%       |_ vdptheory.m
%           | (material props)
%           |_ FourthRank2D.m
%
%%%%%%%%%%%%%%%%%%%%%%%%%%%%%%%%%%%%%%%%%%%%%%%%%%%%%%%%%%%%%%%%%%%%%%%%
%%%%%%%%%%%%%%%%%%%%%%%%%%%%%%%%%%%%%%%%%%%%%%%%%%%%%%%%%%%%%%%%%%%%%%%%
% This function is called by
%
% This Function is responsible for calling vdpsim.m
%
% Parameters:
%   Jd:  [Amp/cm2]   Current Density
%   si_type:  'p' for p-type, 'n' for n-type
%   phi:  [radian]   angle of sensor. I.E. angle from prime
%                       to double primke coordinates
%   p:    [dyne]     Pressure on a circular diaphragm
%
% Results:
%   DeltrNought:      Normalized Resistance Change for 0° Measurement
%   Deltr90:          Normalized Resistance Change for 90° Measurement
%
% Description:  This function chooses from 2 preset sets of pi
% coefficients
% from the literature. It also sets the mechanical material
% properties. It calculates the (biaxial) stress is a
% circular
% diaphragm based on the provided pressure. It then calls
% RV_ROT.m
% to determine the PI and Elastic Modulus Coefficients in the
% double-prime
% system. It passes these calculated values to vdpsim, and
% runs vdpsim 3 times.
% Run 1: Unstressed Resistance. Run 2: Stressed @ 0°. Run 3:
% Stressed @ 90°
%
%
%

```

```

function [DeltRNought,DeltR90]=vdpsimDRIVER(Jd,si_type,phi,p)

format compact

if si_type=='p'
    %%%%%%%%%%%p-type SILICON %%%%%%%%%%%
    pi11=6.6*10^-12;          % * 10 ^-12 dyne/cm^2
    pi12=-1.1*10^-12;        %
    pi44=138.1*10^-12;
    rho=7.8;                 %% p-type [ohm*cm]
    %%%%%%%%%%%
elseif si_type =='n'
    %%%%%%%%%%%n-type SILICON%%%%%%%%%%
    pi11=-102.2*10^-12;      %
    pi12=53.4*10^-12;        % 10^-12 dyne/cm^2
    pi44=-13.6*10^-12;
    rho=11.7;                %% n-type [ohm*cm]
    %%%%%%%%%%%
end

%----- MATERIAL PROPERTIES -----
%-----
E11=1.657*10^12;           %% dyne/(cm^2)
E12=0.639*10^12;
E44=0.796*10^12;
nu=0.27;                   %%Poisson ratio for Silicon
t=0.0020;                  %% Thickness of Diaphragm [cm]
R=0.05;
rfrac=1;                   %% Radius of diaphragm [cm]
r=rfrac*R;                 %% radial position of sensor
%-----
%-----

PIr=[pi11 pi12 0;
     pi12 pi11 0;
     0 0 pi44];

Er=[E11 E12 0;
    E12 E11 0;
    0 0 E44];

alpha1=-7.5;               %% [ohm*cm] Temperature Coefficient
T=0;                       %% Temperature Difference

%STEP 1%
%For a certain value of applied pressure p, calculate the principal
stress

```

```

%components in the sensor coordinate system

%%% CIRCULAR DIAPHRAGM UNDER UNIFORM PRESSURE LOAD %%%%%%%%%%

sig11pp=(-3.*p)./(8*t^2)*((1+nu)*R^2-(3+nu)*r^2)+0.*phi;    %%EQ 7
sig22pp=(-3.*p)./(8*t^2)*((1+nu)*R^2-(1+3*nu)*r^2)+0.*phi; %%EQ 8
sig12pp=0*phi;
sigrpp=[sig11pp;sig22pp;sig12pp];

% sig33pp=-0.*p+0.*phi; %%%% IS THIS CORRECT ??????????
%
% p = external pressure applied to diaphragm dyne/cm^2
% t = thickness of diaphragm cm
% nu = Poisson's ratio of diaphragm material
% R = Diaphragm radius cm
% r = distance from center of diaphragm that VDP is located cm
%
%%%%%%%%%%%%%%%%%%%%%%%%%%%%%%%%%%%%%%%%%%%%%%%%%%%%%%%%%%%%%%%%%%%%%%%%

th=-phi;
PIrpp=RV_ROT(PIr,phi,-pi/4); %
Erpp=RV_ROT(Er,phi,-pi/4); %

delrhopp=rho*PIrpp*sigrpp;
rhopp=[rho;rho;0]+delrhopp;

eprpp=inv(Erpp)*sigrpp;

rho_zero=[rhopp(1); rhopp(2); rhopp(3)];
rho_90= [rhopp(2); rhopp(1); rhopp(3)] ;

%-----
-
% STEP4 %
% Calculate stressed and unstressed resistances. Length ratio AB/CD is
% calculated by using the silicon mechanical properties, Sigxypp, and
% Hooke's law
%-----
--

RPhiNought=vdpsim(Jd,[rho;rho;0],10000);
RPhi90Nought=RPhiNought;

RPhi90Sig=vdpsim(Jd,rho_zero,10000);
RPhiSig=vdpsim(Jd,rho_90,10000);
DeltRNought=(RPhiSig-RPhiNought)./RPhiNought;
DeltR90=(RPhi90Sig-RPhi90Nought)./RPhi90Nought;
DeltNormResDiff=DeltR90 - DeltRNought;

```

RV_ROT.m

```

%
% This function is called by vdpsimDRIVER.m
% CALL STACK
%
%
% vdpboth_psens.m
%   |
%   |_ vdpsim_psens.m
%       |_ vdpsimDRIVER.m
%           | (material props)
%           |_ ****RV_ROT.m*****
%           |_ vdpsim.m
%
%   |_ vdptheory_psens.m
%       |_ vdptheory.m
%           | (material props)
%           |_ FourthRank2D.m
%
%

function [VROT]=RV_ROT(VREF,ENDANG,STARTANG)

DA=STARTANG-ENDANG;
Vr=[(1/2)*(1+cos(2*DA)) (1/2)*(1-cos(2*DA)) sin(2*DA);
     (1/2)*(1-cos(2*DA)) (1/2)*(1+cos(2*DA)) -sin(2*DA);
     (-1/2)*sin(2*DA) (1/2)*sin(2*DA) cos(2*DA)];
VROT=inv(Vr)*VREF*Vr;

```

VDPSIM.M

```

%
% This function is called by vdpsimDRIVER.m
% CALL STACK
%
%
% vdpboth_psens.m
%   |
%   |_ vdpsim_psens.m
%       |_ vdpsimDRIVER.m
%           | (material props)
%           |_ RV_ROT.m
%           |_ ***vdpsim.m***
%
%   |_ vdptheory_psens.m
%       |_ vdptheory.m
%           | (material props)
%           |_ FourthRank2D.m
%
function [Rcd]=vdpsim(Jd,rho,iter)
% Usage is [V,A]=vdpsim(Jd,rho,iter).
% Jd is Current density in units [ Ampere/cm^2 ]
% Rho is Vector with Resistivity Components [rho11;rho22;rho12]
% If Rho is scalar, program computes Isotropic case
% RHO has units [OHM-CM]
% Iter is max number of iterations for Implicit solver

clear A
clear V
%NUMBER OF ELEMENTS - LIMIT 100
XSize=0.01;   %%% cm
YSize=0.01;   %%% cm
nx=40 ;
ny=40 ;      %%% NOTE: NOT YET FULLY DEBUGGED FOR ny != nx
hx=XSize/nx;
hy=YSize/ny;

if hx ~= hy
    disp('WARNING: X AND Y GRID SPACINGS UNEQUAL. SOLUTION MAY BE
INVALID')
end

```



```

    if ind~=nx
    A(s*nx+1:(s+1)*nx,(s+1)*nx+1:(s+2)*nx)=SMULT;
    A((s+1)*nx+1:(s+2)*nx,s*nx+1:(s+1)*nx)=NMULT;
    end
end

b=zeros(nx*ny,1);
Vx=-(rho11+rho12)*(Jd/sqrt(2));
Vy=-(rho12+rho22)*(Jd/sqrt(2));
%b(1)=10
b(1)=2*(hx*Vx*(M(6)+M(3))+hy*Vy*(M(6)+M(2)));
b(2)=M(6)*(2*hy*Vy);
b(nx+1)=M(6)*(2*hx*Vx);
b(nx*ny-2*nx+1)=-2*hx*Vx*M(7);
b(nx*ny-nx+1)=-2*(hx*Vx*(M(7)+M(3))+hy*Vy*(M(7)+M(4)));
b(nx*ny-nx+2)=-2*hy*Vy*M(7);
%b(nx*ny-nx)=-2*h*Vx;
%b(nx*ny)=-4*h*(Vx+Vy);
%b(nx*ny-1)=-2*h*Vy;

x0=0*ones(nx*ny,1);
%x=symmlq(A,b,1E-08,iter);
%x=pcg(-A,-b,1E-08,iter,[],[],x0);
x=lsqr(-A,-b,1E-08,iter,[],[],x0);
row=0;
col=1;
for ind=1:(nx*ny)
    if mod(ind,nx)==1
        row=row+1;
        col=1;
    end
    V(row,col)=x(ind);
    col=col+1;
end

t=0.002;
current1=Jd*t*sqrt(2)/2*hx; % Amp

%J1=K11*(V(2,1)-V(1,1))/hx+K12*(V(1,2)-V(1,1))/hy
%J1=J1*t
%J2=K12*(V(2,1)-V(1,1))/hx+K22*(V(1,2)-V(1,1))/hy
%J2=J2*t
%current2=sqrt(J1^2+J2^2)*0.002 % Amp
Rcd=(V(1,nx)-V(ny,nx))/current1;
%figure
%surf(V')
%V
%%%%% PRIME CALCS %%%%%%
%for ind1=1:(nx-1)
%for ind2=1:(ny-1)
%    VDX(ind1,ind2)=V(ind1,ind2)-V(ind1+1,ind2);
%    VDY(ind1,ind2)=VP(ind1,ind2)-VP(ind1+1,ind2);
%end

```



```

VDPtheory_PSENS.M

% This function is responsible for for running the simulation
% over a range of pressures. These will then be plotted.
%
% CALL STACK
%
%
% vdpboth_psens.m
%
%     |
%     |_ vdpsim_psens.m
%     |   |_ vdpsimDRIVER.m
%     |       | (material props)
%     |       |_ RV_ROT.m
%     |       |_ vdpsim.m
%     |
%     |_ ****vdptheory_psens.m****
%     |   |_ vdptheory.m
%     |       | (material props)
%     |       |_ FourthRank2D.m
%
%
clf
ANGLE=pi/4;

hold off
figure
[a,b]=vdptheory(1,'n',-1,-1);
set(gca,'LineStyle',':')
hold on
set(gca,'LineWidth',2)
[a,b]=VDPtheory(1,'p',-1,-1);
title({'Normalized Resistance Change';'Angular dependence of Sensor on
Wafer';
'n-Type and p-Type silicon'});
legend('n-Type','p-Type')
hold off
press_theory=0:100000:2000000;
for i=1:size(press_theory,2)

[pNRCTtheory(i,1),pNRCTtheory(i,2)]=VDPtheory(1,'p',ANGLE,press_theory(i)
);

[nNRCTtheory(i,1),nNRCTtheory(i,2)]=VDPtheory(1,'n',ANGLE,press_theory(i)
);
end

```

```

VDP THEORY.M

% This function is called from vdptheory_psens.m
%
% This function calculates the theoretical values of
% the 2D pressure sensitivity by calculating the
% biaxial stress load that would arise in a circular diaphragm
%
%
% CALL STACK
%
%
% vdpboth_psens.m
%   |
%   |_ vdpsim_psens.m
%       |_ vdpsimDRIVER.m
%           | (material props)
%           |_ RV_ROT.m
%           |_ vdpsim.m
%
%   |_ vdptheory_psens.m
%       |_ ****vdptheory.m****
%           | (material props)
%           |_ FourthRank2D.m
%
%
function
[DeltRNought, DeltR90, sig11pp, sig22pp]=vdptheory(rfrac, si_type, phi, p)
I=1;
%rfrac=0.5;
if phi == -1
phi=0:pi/180:2*pi; % Angle from x' axes to x'' axes
end

if p==-1
p=1000000; %% [dyne/cm^2] 10^6 dyne/cm^2 = 100kPa
end

if si_type=='p'
%%%%%%%%%%%%p-type SILICON
%%%%%%%%%%%%
pi11=6.6*10^-12; % 10^-12 dyne/cm^2
pi12=-1.1*10^-12;
pi44=138.1*10^-12;
rho=7.8;
%%%%%%%%%%%%
%%
elseif si_type=='n'
%%%%%%%%%%%%n-type
%%%%%%%%%%%%
SILICON%%%%%%%%%%%%
pi11=-102.2*10^-12;
pi12=53.4*10^-12; % 10^-12 dyne/cm^2
pi44=-13.6*10^-12;

```

```

rho=11.7;          %% n-type [ohm*cm]
%%%%%%%%%%%%%%%%%%%%%%%%%%%%%%%%%%%%%%%%%%%%%%%%%%%%%%%%%%%%%%%%%%%%%%%%
%
end
E11=1.657*10^12;  %% dyne/(cm^2)
E12=0.639*10^12;
E44=0.796*10^12;
nu=0.27;          %%Poisson ratio for Silicon
t=0.0020;        %% Thickness of Diaphragm [cm]
R=0.05;          %% Radius of diaphragm [cm]
r=rfrac*R;       %% radial position of sensor

alpha1=-7.5;     %% [ohm*cm]
T=0;
%STEP 1%
%For a certain value of applied pressure p, calculate the principal
stress
%components in the sensor coordinate system

%% CIRCULAR DIAPHRAGM UNDER UNIFORM PRESSURE LOAD %%%%%%%%%%
sig11pp=(-3.*p)./(8*t^2)*((1+nu)*R^2-(3+nu)*r^2)+0.*phi;    %%EQ 7
sig22pp=(-3.*p)./(8*t^2)*((1+nu)*R^2-(1+3*nu)*r^2)+0.*phi; %%EQ 8
sig12pp=0*phi;
sig33pp=-0.*p+0.*phi;   %%%% IS THIS CORRECT ??????????
%
% p = external pressure applied to diaphragm
% t = thickness of diaphragm
% nu = Poisson's ratio of diaphragm material
% R = Diaphragm radius
% r = distance from center of diaphragm that VDP is located
%
%%%%%%%%%%%%%%%%%%%%%%%%%%%%%%%%%%%%%%%%%%%%%%%%%%%%%%%%%%%%%%%%%%%%%%%%

%STEP 2%
%Transform the stresses from sensor coordinate system (double primed)
%to the wafer flat coordinate system (primed)

%%%%%%%% ROTATE SENSOR STRESSES (TANG AND RAD) BACK TO WAFER SYSTEM
th=-phi;
sig11p=(1/2).*(sig11pp+sig22pp)+(1/2).*(sig11pp-
sig22pp).*cos(2.*th)+sig12pp.*sin(2.*th);
sig22p=(1/2).*(sig11pp+sig22pp)-(1/2).*(sig11pp-
sig22pp).*cos(2.*th)-sig12pp.*sin(2.*th);
sig12p=-(1/2).*(sig11pp-sig22pp).*sin(2.*th)+sig12pp.*cos(2.*th);
sig33p=sig33pp;
%%%%%%%%%%%%%%%%%%%%%%%%%%%%%%%%%%%%%%%%%%%%%%%%%%%%%%%%%%%%%%%%%%%%%%%%

% STEP 3 %
%Calculate the resistivity components
%
%%%%%%%%% IN PLANE COMPONENTS OF RESISTIVITY TENSOR %%%%%%%%%% EQ
(6)
%%%%%%%%% IN [1 1 0]

```

```

    rho11p=rho*(1+(1/2)*(pi11+pi12+pi44)).*sig11p+(1/2).*(pi11+pi12-
pi44).*sig22p+pi12.*sig33p+alpha1*T);
    rho22p=rho*(1+(1/2)*(pi11+pi12-
pi44)).*sig11p+(1/2).*(pi11+pi12+pi44).*sig22p+pi12.*sig33p+alpha1*T);
    %rho12p=rho*(pi44*sig12p); %This might be wrong??
    rho12p=rho*((pi11-pi12)*sig12p);
    %%%%%%%%%%%%%%%%%%%%%%%%%%%%%%%%%%%%%%%%%%%%%%%%%%%%%%%%%%%%%%%%%%%%%%%%%
    %% RESISTIVITY COMPONENTS IN ROTATED DOUBLE PRIMED SENSOR
COORDINATE SYSTEM %%%%%%%%%

rho11pp=rho11p.*(cos(phi)).^2+rho12p.*sin(2*phi)+rho22p.*(sin(phi)).^2;
rho22pp=rho11p.*(sin(phi)).^2-
rho12p.*sin(2*phi)+rho22p.*(cos(phi)).^2;
rho12pp=(rho11p-rho22p)/2.*sin(2.*phi)+rho12p.*cos(2*phi);
    %%%%%%%%%%%%%%%%%%%%%%%%%%%%%%%%%%%%%%%%%%%%%%%%%%%%%%%%%%%%%%%%%%%%%%%%% EQ
(5)

% STEP4 %
% Calculate stressed and unstressed resistances. Length ratio AB/CD is
% calculated by using the silicon mechanical properties, Sigxypp, and
% Hooke's law

E=zeros(6,6);
E(1:3,1:3)=[E11 E12 E12; E12 E11 E12; E12 E12 E11];
E(4:6,4:6)=E44*eye(3);
Ep=FourthRank2D(E,0,45);
C=inv(Ep);

epp=C*[sig11p;sig22p;sig33p;0*sig12p;0*sig12p;sig12p];
[sig11pp;sig22pp;sig33pp;0*sig12pp;0*sig12pp;sig12pp];
ep11p=epp(1);
ep22p=epp(2);
ep12p=epp(6);
ep11pp=(1/2).*(ep11p+ep22p)+(1/2).*(ep11p-
ep22p).*cos(2.*phi)+ep12p.*sin(2.*phi);
ep22pp=(1/2).*(ep11p+ep22p)-(1/2).*(ep11p-ep22p).*cos(2.*phi)-
ep12p.*sin(2.*phi);
ep12pp=-(1/2).*(ep11p-ep22p).*sin(2.*phi)+ep12p.*cos(2.*-phi);

lratio=(1+ep11pp)/(1+ep22pp);

SUMadbc=1;
SUMabcd=1;
premult=-(8/(pi*t)).*sqrt(rho11pp.*rho22pp); %%abs
iter=10;
inside=lratio.*sqrt(rho11pp./rho22pp); %%abs
    for index1=0:iter
        SUMadbc=SUMadbc.*tanh(inside.*(2*index1+1)*(pi/2));
        SUMabcd=SUMabcd.*tanh((1./inside).*(2*index1+1)*(pi/2));
    end
Radbc=premult.*log(SUMadbc);
RPhi90Sig=Radbc;
Rabcd=premult.*log(SUMabcd);
RPhiSig=Rabcd;

```

```
RPhiNought=rho*log(2)/(pi*t);
RPhi90Nought=RPhiNought;
DeltRNought=(RPhiSig-RPhiNought)./RPhiNought;
DeltR90=(RPhi90Sig-RPhi90Nought)./RPhi90Nought;
DeltNormResDiff=DeltRNought - DeltR90;

if size(phi,2)>1
    polar(phi,DeltNormResDiff);
end
```

```

FOURTHRANK2D.M

% This function rotates a reduced fourth rank tensor in 2D
%
% The tensor values will be in 6x6 matrix form.
% CALL STACK
%
%
% vdpboth_psens.m
%
%   |
%   |_ vdpsim_psens.m
%   |   |_ vdpsimDRIVER.m
%   |       | (material props)
%   |       |_ RV_ROT.m
%   |       |_ vdpsim.m
%   |
%   |_ vdptheory_psens.m
%   |   |_ vdptheory.m
%   |       | (material props)
%   |       |_ *****FourthRank2D.m*****
%
function [TENS]=FourthRank2D(TENSREF,STARTANG,ENDANG)

STARTANG=STARTANG*pi/180;
ENDANG=ENDANG*pi/180;
DA=ENDANG-STARTANG;

c=cos(DA);
s=sin(DA);

K=[c^2 s^2 0 0 0 2*c*s;
   s^2 c^2 0 0 0 -2*c*s;
   0 0 1 0 0 0;
   0 0 0 c s 0;
   0 0 0 -s c 0;
  -c*s c*s 0 0 0 c^2-s^2];

TENS=K*TENSREF*K';

```

APPENDIX B

ANSYS INPUT FILES

```

! 2D Analysis of Serpentine Piezo resistor
!
!
!/INPUT, 'c:\ansyswork\2D\SERP-2D_rev3','inp'
finish
/cwd,c:\ansyswork\2D
/clear,nostart
/title, Serpentine piezoresistive element, uMKS system of units

ELEMDOUBLE=2
SOLVEFLAG=1
ANGLE=0
PRESSUREX=0 ! MPa
PRESSUREY=0
PHI=1
!
!
! GEOMETRIC PARAMETERS
!
!
W=125 ! width of piezoresistor, um
L=W ! length of piezoresistor, um
!b=23 ! width of signal-conducting arm, um
!a=2*b ! length of signal-conducting arm, um
S=2*L ! size of square diaphragm, um

!
!
! MATERIAL PROPERTIES
!
!
! Stiffness, MN/m^2
! [c11 c12 c12 0 ]
! [c12 c11 c12 0 ]
! [c12 c12 c11 0 ]
! [ 0 0 0 c44]
!
c11= 165.7e3
c12= 63.9e3
c44= 79.6e3
/com,
/com, Resistivity (p-type Si), Ohm*um
rho=7.8e-8
!rho= 78000
!/com, Piezoresistive coefficients (p-type Si), (MPa)^(-1)
!/com, [p11 p12 p12 0 ]
!/com, [p12 p11 p12 0 ]
!/com, [p12 p12 p11 0 ]
!/com, [ 0 0 0 p44]
!/com,
p11=6.6e-5
p12=-1.1e-5
p44=138.1e-5
!
!

```

```

!
! LOADING CONDITIONS
! _____
!
!
/com, Pressure load, MPa
p=PRESSUREX ! MPa
/com, Source voltage, Volt
Vs=5
/nopr

! _____
!
! ELEMENT TYPES
! _____
!
!
/prep7
et,1,PLANE223,101          ! piezoresistive element type, plane
stress
et,2,PLANE183             ! structural element type, plane stress

! _____
!
! COORDINATE SYSTEMS
! _____
!                               ! Specify material orientation

local,11,,,,,ANGLE
local,13,,,,,-45          ! X-axis along [110] direction. MATERIAL
COORDINATE SYSTEM

! _____
!
! CREATE OTHER COORD SYS
! _____
!
      CSYS,11              ! CONSTRUCTION AXIS FOR RESISTOR
AREA

      CLOCAL,12,0,0,0,0,90,0,0          ! DEFINE COORD SYS 12
FOR 90 ANGLE (PHI=1)
      CSYS,11

      CLOCAL,16,0,0,0,0,90,90,0        ! DEFINE COORD SYS 16
FOR 0 ANGLE WP
      CSYS,11

      CLOCAL,17,0,0,0,0,180,90,0       ! DEFINE COORD SYS 17
FOR 90 ANGLE WP
      CSYS,11

! _____
!
! ANISOTROPIC MATERIAL PROPERTIES
! GENERATE MATERIAL IN CSYS,13

```

```

! _____
!
! Specify material properties:
tb,ANEL,1,,,0      ! anisotropic elasticity matrix
tbda,1,c11,c12,c12
tbda,7,c11,c12
tbda,12,c11
tbda,16,c44

mp,RSVX,1,rho      ! resistivity

tb,PZRS,1          ! piezoresistive stress matrix
tbdata,1,p11,p12,p12
tbdata,7,p12,p11,p12
tbdata,13,p12,p12,p11
tbdata,22,p44

! _____
!
! CREATE GEOMETRIES
! _____
!

numberoflegs=4      ! Number of piezoresistive legs. Must be
Even >=2
LW=W/(2*numberoflegs-1) ! LW = LegWidth
CW=W/10             ! CW = interConnectWidth
csys,11+PHI        !

k,1,-W/2,W/2
k,2,W/2,W/2
k,3,W/2,W/2-LW
k,4,-W/2,W/2-LW
k,5,W/2-CW,W/2-LW
k,6,W/2, W/2-LW
k,7,W/2, W/2-2*LW
k,8,W/2-CW,W/2-2*LW
k,9,-W/2,W/2-3*LW
k,10,-W/2+CW,W/2-3*LW
k,11,-W/2+CW,W/2-4*LW
k,12,-W/2,W/2-4*LW
a,1,2,3,4
a,5,6,7,8
*IF,numberoflegs, gt,2,then
a,9,10,11,12
*ENDIF

agen,numberoflegs,1,1,1,0,-2*LW,0
agen,numberoflegs/2,2,2,1,0,-4*LW,0
*IF,numberoflegs, gt,2,then
agen,numberoflegs/2-1,3,3,1,0,-4*LW,0
*ENDIF

```

```

aadd,all
*get, resistorarea,area,0,NUM,MAXD

asel,all
csys,0
rect,-S/2,S/2,-S/2,S/2      ! Define Structural area in GLOBAL
coordinates

! _____
!
! CREATE GEOMETRIES
! _____
!
csys,11
tol=0.001                    ! Mesh areas:
PAD=L/10
aovlap,all
outarea=2
esys,13
type,1
esize,LW/ELEMDOUBLE
mshape,0,2D                  ! use triangles
amesh,resistorarea
type,2
esize,S/20
amesh,outarea

! _____
!
! CREATE ELECTRICAL BC's
! _____
!
csys,11+PHI                  ! Apply electrical BC
nsel,s,loc,x,-W/2-tol,-W/2+tol
nsel,r,loc,y,W/2-LW-tol,W/2+tol
cp,1,volt,all                ! left electrode:
*get,n1,node,0,num,min       ! get master node
d,n1,volt,Vs                  ! apply source voltage Vs

nsel,s,loc,x,-W/2-tol,-W/2+tol
nsel,r,loc,y,-W/2+LW+tol,-W/2-tol
d,all,volt,0                  ! ground right electrode

! _____
!
! CREATE STRUCTURAL BC's
! _____
!
csys,0                        ! Apply structural BC
nsel,s,loc,x,-S/2

```

```

d,all,ux,0
nsel,s,loc,y,-S/2
d,all,uy,0

! _____
!
! DEFINE PATH POINTS
! _____
!
CSYS,12-PHI

nsel,s,loc,x,0
nsel,r,loc,y,W/2+LW/2
*get,NTOP,node,0,num,min
nsel,s,loc,x,0
nsel,r,loc,y,W/2-LW/2
*get,NBOTTOM,node,0,num,min
nsel,all
CSYS,11

! _____
!
! CREATE PRESSURE LOAD
! _____
!
CSYS,0
nsel,s,loc,x,S/2
sf,all,pres,-pressurex
nsel,s,loc,y,S/2
sf,all,pres,-pressurey ! pressure load
csys,11
nsel,all

/psc,u,,1
/psc,volt,,1
/psc,cp,,1
/pnum,type,1
/number,1
eplot
fini
*IF, solveflag,eq,0,then
/EOF
*ENDIF
/solu                                ! Solution

antype,static
cvtol,amps,1,1.e-3                    ! Optional to prevent a warning message

solve

```

```
/post1
```

```
! _____
!  
! PLOT SOLUTION  
! _____
!
```

```
plesol,volt  
/PLOPTS,DATE,0  
/TRIAD,OFF  
/CONTOUR,1,20,AUTO,,  
CSYS,11+PHI
```

```
! _____
!  
! CREATE INTEGRATION PATHS  
! _____
!
```

```
nselect,s,loc,x,-W/2-tol,-W/2+tol  
nselect,r,loc,y,W/2-tol,W/2+tol  
*get,NODEPBOTTOM,node,0,num,min  
nselect,s,loc,x,-W/2-tol,-W/2+tol  
nselect,r,loc,y,W/2-LW-tol,W/2+tol  
*get,NODEPTOP,node,0,num,min  
nselect,all
```

```
PATH,PATHCUT1,2,30,80,  
PPATH,1,NODEPBOTTOM  
PPATH,2,NODEPTOP
```

```
! _____
!  
! INTEGRATE THE CURRENT  
! _____
!
```

```
psel,s,PATHCUT1  
pdef,mapdjcx,jc,x,NOAV  
!pmap,uniform,MAT  
PCALC,INTG,intcurrx,MAPDJCX,S  
PAGET,INTarrx, TABLE  
icurry=20*INTarrx(81,6)
```

```
PATH,PATHCUT2,2,30,80,  
PPATH,1,NODEPBOTTOM  
PPATH,2,NODEPTOP  
psel,s,PATHCUT2  
pdef,mapdjcy,jc,y,NOAV  
PCALC,INTG,intcurry,MAPDJCY,S  
PAGET,INTarry, TABLE  
icurrx=20*INTarry(81,6)
```

```
integratedcurrent=(icurrx**2+icurry**2)**(0.5)*1e-12  
RES=(Vs-0)/integratedcurrent  
/COM, Integrated Current = %integratedcurrent% AMPS  
/COM, RESISTANCE (ANSYS) = %RES% OHMS  
/plopts,logo,0  
plvect,jc,sum,,,vect,
```

2D ANALYSIS OF VDP SENSITIVITY

```

!
! 2D VDP ANALYSIS
!
!/INPUT, 'c:\ansyswork\2D\VDP-2D_rev3','inp'
!
!

/cwd,c:\ansyswork\2D\
finish
/clear,nostart
/plopts,logo,0
solveflag=1
ANGLE=0
PRESSUREY=0
PRESSUREX=25!0.27*PRESSUREY    !! STRESS UNITS: MPa

PHI=0          ! PHI = 0 : VOLTAGE APPLIED ON LEFT
!
!
! GEOMETRIC PARAMETERS
!
!
W=125          ! width of piezoresistor, um
L=W            ! length of piezoresistor, um
!b=23         ! width of signal-conducting arm, um
!a=2*b        ! length of signal-conducting arm, um
S=2*L        ! size of square diaphragm, um
!
!
! MATERIAL PROPERTIES
!
!
! Stiffness, MN/m^2
! [c11 c12 c12 0 ]
! [c12 c11 c12 0 ]
! [c12 c12 c11 0 ]
! [ 0 0 0 c44]
!
c11= 165.7e3
c12= 63.9e3
c44= 79.6e3
!
! Resistivity (p-type Si), Ohm*um
rho=7.8e-8 ! TOhm*um
!rho= 78000
!
! Piezoresistive coefficients (p-type Si), (MPa)^(-1)
! [p11 p12 p12 0 ]
! [p12 p11 p12 0 ]
! [p12 p12 p11 0 ]
! [ 0 0 0 p44]
!

```

```

p11=6.6e-5
p12=-1.1e-5
p44=138.1e-5
!
! _____
!
! LOADING CONDITIONS
! _____
!
p=PRESSUREX          !Pressure load, MPa
Vs=5                 !Source voltage, Volt
tol=0.001                               ! Mesh areas:
PAD=L/40

/nopr
/prep7
! _____
!
! ELEMENT TYPES
! _____
!
et,1,PLANE223,101      ! piezoresistive element type, plane
stress
et,2,PLANE183         ! structural element type, plane stress
! _____
!
! COORDINATE SYSTEMS
! _____
!
! Specify material orientation
local,11,,,,,ANGLE
csys,11
local,13,,,,,-45      ! X-axis along [110] direction

! _____
!
! CREATE OTHER COORD SYS
! _____
!
      CSYS,11

      CLOCAL,12,0,0,0,0,90,0,0          ! DEFINE COORD SYS 12
FOR 90 ANGLE
      CSYS,11

      CLOCAL,16,0,0,0,0,90,90,0        ! DEFINE COORD SYS 16
FOR 0 ANGLE WP
      CSYS,11

      CLOCAL,17,0,0,0,0,180,90,0       ! DEFINE COORD SYS 17
FOR 90 ANGLE WP
      CSYS,11

```

```

! _____
!
! ANISOTROPIC MATERIAL PROPERTIES
!   GENERATE MATERIAL IN CYSY,12
! _____
!
csys,13                ! Specify material properties:
tb,ANEL,1,,0          ! anisotropic elasticity matrix
tbda,1,c11,c12,c12
tbda,7,c11,c12
tbda,12,c11
tbda,16,c44

mp,RSVX,1,rho         ! resistivity

tb,PZRS,1             ! piezoresistive stress matrix
tbdata,1,p11,p12,p12
tbdata,7,p12,p11,p12
tbdata,13,p12,p12,p11
tbdata,22,p44

! _____
!
! CREATE GEOMETRIES
! _____
!
csys,11                ! Define piezoresistor area:

!rect,-W/2,W/2,-W/2,W/2
k,1,-W/2,-W/2
k,2,W/2,-W/2
k,3,W/2,W/2
k,4,-W/2,W/2
a,1,2,3,4
csys,0                 ! Define structural area:
rect,-S/2,S/2,-S/2,S/2

aovlap,all
esys,13
type,1
esize,W/20
mshape,0,2D           ! use SQUARES
amesh,1
type,2
esize,S/40
amesh,3

! _____
!
! CREATE ELECTRICAL BC's
! _____
!

```

```

csys,12-PHI                                ! Apply electrical BC

nsl,s,loc,x,-L/2-tol,-L/2+PAD+tol
nsl,r,loc,y,W/2-PAD-tol,W/2+tol
cp,1,volt,all                               ! left electrode:
*get,nl,node,0,num,min                      ! get master node
d,nl,volt,Vs                                ! apply source voltage Vs

nsl,s,loc,x,L/2-PAD-tol,L/2+tol
nsl,r,loc,y,W/2-PAD-tol,W/2+tol
cp,2,volt,all
*get,nm,node,0,num,min
d,nm,volt,0 !-Vs                            ! ground right electrode

nsl,s,loc,x,-L/2-tol,-L/2+PAD+tol
nsl,r,loc,y,-L/2-tol,-L/2+PAD+tol
cp,3,volt,all                               ! top electrode:
*get,nt,node,0,num,min                     ! get master node

nsl,s,loc,x,W/2-PAD-tol,W/2+tol
nsl,r,loc,y,-W/2-tol,-W/2+PAD+tol
cp,4,volt,all                               ! bottom electrode:
*get,nb,node,0,num,min                     ! get master node

nsl,all

! _____
!
! CREATE STRUCTURAL BC's
! _____
!

csys,0                                       ! Apply structural BC
nsl,s,loc,x,-S/2
dsym,symm,x
nsl,s,loc,y,-S/2
dsym,symm,y

! _____
!
! CREATE PRESSURE LOAD
! _____
!

nsl,s,loc,y,S/2
sf,all,pres,-pressurey
nsl,s,loc,x,S/2
sf,all,pres,-pressurex
nsl,all

CSYS,12-PHI

nsl,s,loc,x,0
nsl,r,loc,y,W/2
*get,NTOP,node,0,num,min

```

```

nset,s,loc,x,0
nset,r,loc,y,-W/2
*get,NBOTTOM,node,0,num,min
nset,all
CSYS,11

/pcb,u,,1
/pcb,volt,,1
/pcb,cp,,1
/pnum,type,1
/number,1
eplot
fini

/solu                                ! Solution

antype,static
cnvtol,amps,1,1.e-3                 ! Optional to prevent a warning message
*IF, solveflag,eq,0,then
/EOF
*ENDIF

solve
fini

/post1

! _____
!
! PLOT SOLUTION
! _____
!

plesol,volt
/PLOPTS,DATE,0
/TRIAD,OFF
/CONTOUR,1,20,AUTO,,
CSYS,12-PHI

! _____
!
! CREATE INTEGRATION PATHS
! _____
!

PATH,PATHCUT1,2,30,80,
PPATH,1,NBOTTOM
PPATH,2,NTOP
psel,s,PATHCUT1
pdef,mapdjcxc,jc,x,NOAV
!pmap,uniform,MAT
PCALC,INTG,intcurrxc,MAPDJCX,S
PAGET,INTarrxc, TABLE

```

```
icurrx=20*INTarrx(81,6)

PATH,PATHCUT2,2,30,80,
PPATH,1,NBOTTOM
PPATH,2,NTOP
psel,s,PATHCUT2
pdef,mapdjcy,jc,y,NOAV
PCALC,INTG,intcurry,MAPDJCY,S
PAGET, INTarry, TABLE
icurry=20*INTarry(81,6)

integratedcurrent=(icurrx**2+icurry**2)**(0.5)*1e-12

voltagediff=volt(nt)-volt(nb)
RES=voltagediff/integratedcurrent
/COM, Voltage Out (ANSYS) = %voltagediff% Volts
/COM, CURRENT (ANSYS) = %integratedcurrent% Amps
/COM, RESISTANCE (ANSYS) = %RES% Ohms
```

PRESSURE DIAPHRAGM INPUT FILE

```
!This file creates A square diaphragm of the dimensions that we have
specified for
!the masks we have ordered. It solves the displacement and stress of
the diaphragm and
!then runs ____ VDP_sub.inp ____ which takes displacement data to do a
refined
!submodel analysis.
!
!/INPUT,'c:\ANSYSWork\3D\Diaph-3D_rev8','inp',,, 0
!
```

```
finish
/begin
/clear, nostart
/cwd,c:\ansyswork\3D\
/filename,'diaphragmjob','DB',1
/UNITS,SI
/prep7
```

```
!
!-----
!   DIMENSIONS
! [F] = uNewton
! [L] = um
! [T] = seconds
! [P] = uNewton/um^2
! [pi] = um^2 / uNewton
!
!-----
!
```

```
PARRES, CHANGE, '__saved_geometric_parameters','inp'
```

```
!
!-----
!   MATERIAL PARAMETERS
!-----
!
!si_EX      = 47E07
!si_PRXY    = 0.27
!si_resistance = 78000 !7.8E-04
!si_ntyperesistance=1000000 ! 100
!
!pi11 =      6.6E-05      ! UNITS OF (MPa)-1 ! UNPRIMED
!pi12 =     -1.1E-05
!pi13 = pi12
!pi33 = pi11
!pi44 =     138.1E-05
!pi66 = pi44
!
!E11 =     165.7E03      ! UNPRIMED
!E12 =      63.9E03
```

```

!E13      =  E12
!E33     =  E11
!E44     =    79.6E03
!E66     =  E44

!
!-----
! GEOMETRIC PARAMETERS !
!-----
!

!g_diaphxy=10000          ! DIAPHRAGM DIMENSION
!g_basexy=1000           ! BASE DIMENSION (Amount frame
extends beyond diaphragm)
!g_diaphthickness=200    ! DIAPHRAGM THICKNESS
!g_basethickness=325     ! BASE HEIGHT (Additional height
the base provides)
!g_height=g_basethickness+g_diaphthickness      ! Total height
!g_vdpdepth=20
!g_resistorangle=0
!g_width=g_diaphxy+g_basexy
!tol=0.001

!XOFFSET=0
!YOFFSET=g_basexy
!-----
!
! CREATE OTHER COORD SYS
!-----
local,11,0,XOFFSET,YOFFSET,0,0,0,0
csys,11
clocal,13,,,,,-45 !!! X-AXIS ALONG [1 1 0] DIR

CSYS,11
CLOCAL,12,0,0,0,0,90,0,0      ! DEFINE COORD SYS 20 FOR 90 ANGLE

CSYS,11
CLOCAL,16,0,0,0,0,90,90,0     ! DEFINE COORD SYS 16 FOR 0 ANGLE
WP (CUTS 11)

CSYS,11
CLOCAL,17,0,0,0,0,180,90,0    ! DEFINE COORD SYS 17 FOR 90 ANGLE
WP (CUTS 12)
csys,11

csys,0                        ! RESET TO GLOBAL COORDS

!!! USE CYS 15 FOR MAKING DIAPHRAGM GEOMETRY
!!! ORIGIN OF CSYS 15 SITS AT CENTER OF DIAPHRAGM
!!! 15 IS OFFSET FROM GLOBAL ORIGIN SUCH THAT AFTER CREATING
DIAPHRAGM GEOM IN 15
!!! THE VERY EDGE OF DIAPHRAGM SUPPORT SITS AT GLOBAL ORIGIN AND
THE
!!! DIAPHRAGM ATTACHMENT TO SUPPORT BASE IS AT (0, g_basexy, 0)
IN GLOBAL COORDS

```

```

local,15, 0, 0, g_diaphxy+g_basexy, 0,180, 0 , 0, 0 ,0
csys,13
!
!-----
!
!-----
!
! MATERIAL PROPERTIES
!-----
!
!#### DEFINE RESISTOR MATERIAL - MATERIAL 1
MP,RSVX,1,si_p_rho
TB,PZRS,1, , ,0          ! PI COEFFICIENTS

TBDATA,1, pi11,pi12,pi13 ,0,0,0
TBDATA,7, pi12,pi11,pi13 ,0,0,0
TBDATA,13,pi13,pi13,pi33 ,0,0,0
TBDATA,19,0,0,0, pi44,0,0
TBDATA,25,0,0,0, 0,pi44,0
TBDATA,31,0,0,0, 0,0,pi66

TB,ANEL,1,0, ,0          ! ANISOTROPIC ELASTICITY
! COEFFICIENTS
TBDATA,1,c11,c12,c13,0, 0, 0
TBDATA,7, c11,c13,0, 0, 0
TBDATA,12, c33,0, 0, 0
TBDATA,16, c44,0, 0
TBDATA,19, c44,0
TBDATA,21, c66

!-----
!
! LOAD PARAMETERS
!-----
!
l_pressure=0.1      !! 100kpa = 0.100 uN/um^2

!-----
!
! DEFINE KEYPOINTS
!-----
!
CSYS,15

k,101, g_width, 0 ,0
k,102 , g_width, g_width ,0
k,103, -g_width, g_width ,0
k,104, -g_width, 0 ,0
k,105, g_diaphxy, 0 ,0
k,106, g_diaphxy, g_diaphxy ,0
k,107, -g_diaphxy, g_diaphxy ,0

```

```

k,108, -g_diaphxy, 0 ,0
k,109,  g_width  , g_diaphxy ,0
k,110,  g_diaphxy, g_width  ,0
k,111, -g_diaphxy, g_width  ,0
k,112, -g_width,   g_diaphxy ,0

```

```
!KGEN, ITIME, NP1, NP2, NINC, DX, DY, DZ, KINC, NOELEM, IMOVE
```

```

kgen,2,101,112,1,0,0,-g_diaphthickness,100,0,0
kgen,2,101,112,1,0,0,-g_height,200,0,0

```

```

!-----
!
!       DEFINE AREAS
!-----
!

```

```

a,101,102,103,104 ! AREA 1 - ENTIRE TOP SURFACE
a,105,106,107,108 ! AREA 2 - DIAPHRAGM ONLY AREA
asba,1,2,,keep,keep ! AREA 3 - SUPPORT BASE AREA

```

```

!-----
!
! DEFINE VOLUME ELEMENT
!-----
!
!

```

```
et,1,solid187
```

```

!-----
!
! GENERATE VOLUMES
!-----
!

```

```

asel,all
voffst,1,-g_diaphthickness,1000 ! VOLUME 1 - TOP VOLUME -
TRYING TO GET RID OF STRESS CONC

```

```

*get,lastarea,area,,count
aoffst,3,-g_diaphthickness,2000 ! MOVE SUPPORT BASE AREA 4
INTO POSITION
voffst,lastarea+1,-g_basethickness,1000 ! VOLUME 2 - SUPPORT BASE
VOLUME
vadd,1,2 ! VOLUME 3 - COMBINE BASE AND TOP
vdele,1,2,1

```

```

aclear,all
vsel,all
mshkey,0 ! USE MAPPED MESHING (1) FREE MESHING (0)
mshape,1,3D ! USE TRIANGLE ELEMENTS (1), SQUARE
ELEMENTS (0)
esize,g_diaphxy/20
esys,13

```

```

vmesh,all
aclear,all
csys,15
!
!
! IMPROVE VIEW
!
!
esel,all
eplot
/VIEW, 1, 0.301941323934 , 0.679419448262 , -0.668745579593
/ANG, 1, 160.139335315
/REPLO
!
!
! IMPOSE FIXED BASE BC
!
!
nselect,s,loc,z,-g_height-tol,-g_height+tol
d,all,all,0
!
!
! IMPOSE SYMMETRY AT X=0
!
!
nselect,s,loc,y,-tol,tol
dsym,symm,y,0
!
!
! APPLY SURFACE LOAD AT Z=0
!
!
nselect,s,loc,z,-tol,tol
sf,all,PRES,1_pressure
nselect,all
!
!
! SOLVE
!
!
csys,0

/solu
!ANTYPE,static          !!! UNCOMMENT THESE LINES
!NLGEOM, ON             !!! FOR STRESS STIFFENING
!SOLCONTROL, ON
!SSTIF,ON
!NSUBST,10,20,1,ON

solve
/post1
pldisp
/VIEW, 1, 0.843895611584 , 0.479209951639 , 0.241242655846
/ANG, 1, -98.1598848639

```

```
/REPLO  
!  
!  
!      BEGIN SUBMODELING  
!  
!  
save,'diaphragmjob','db',,all
```

SUBMODELED VDP INPUT FILE

```

!!! The goal of this input file is to determine the Normalized
Resistance
!!! Change Difference (NRCD) For a square VDP. This file creates the
!!! VDP geometry and submodel area, and calls Diaph-3D_###.inp to
determine
!!! the submodeling boundary conditions/
!!!
!!! The current goal is to match theoretical and MATLAB finite
difference data.
!!!
!!! REVISION LIST:
!!! THIS MODIFICATION USES VOLTAGE DOF INSTEAD OF AMPS FORCE
!!! Changed value of si_EX from 47E07 to MATLAB values. Anisotropic
matrix
!!! - PIEZORESISTIVE MATRIX WAS IN WRONG CSYS. NOW ROTATED 45° TO
PRIME COORDS
!/INPUT,'c:\ANSYSWork\3D\VDP-3Dsub_rev8','inp',,, 0

/cwd,c:\ansyswork\3D\
finish
/clear,nostart
/filename,'VDPsubmodel','DB',1
/prep7

MASS_RUN_FLAG=0  !! IF THIS EQUALS 1 THEN IT MEANS THIS FILE IS BEING
MANAGED FROM VDP-3D_massrun_rev?.inp

!
!-----
! DIMENSIONS
! [F] = uNewton
! [L] = um
! [T] = seconds
! [P] = uNewton/um^2
! [pi] = um^2 / uNewton
! [Ohm] = TOhm
! [Amp] = pA
!
!-----
!
! MATERIAL PARAMETERS
!-----

si_p_rho=7.8e-8
pi11 = 6.6E-05 ! UNITS OF (MPa)-1 ! UNPRIMED
pi12 = -1.1E-05
pi13 = pi12
pi33 = pi11
pi44 = 138.1E-05
pi66 = pi44

c11 = 165.7E03 ! UNPRIMED
c12 = 63.9E03

```

```

c44 = 79.6E03
c13 = c12
c33 = c11
c66 = c44

! _____
!
! GEOMETRIC PARAMETERS !
!
! _____ALREADY DEFINED FROM PARRES_____
!
PHI=0
ANGLE=0
g_diaphxy=5000 ! DIAPHRAGM DIMENSION (HALF WIDTH IE FROM
CENTER TO EDGE)
g_basexy=1000 ! BASE DIMENSION
g_diaphthickness=200 ! DIAPHRAGM THICKNESS
g_basethickness=325 ! BASE HEIGHT
g_height=g_basethickness+g_diaphthickness
g_submodelwidth=400
g_submodellength=g_submodelwidth
g_submodeldepth=g_diaphthickness/2
g_vdpsize=125
g_vdpdepth=20 ! Diffusion depth of VDP
g_vdpangle=ANGLE ! Rotation angle of VDP
g_width=g_diaphxy+g_basexy
tol=0.001
XOFFSET=0
YOFFSETrel=120 !! @@ THIS IS THE CENTER OF THE SUBMODEL SECTION
=g_basexy: SUBMODEL SECTION CENTERED AT DIAPHRAGM EDGE
YOFFSET=g_basexy+YOFFSETrel

! _____
!
! LOAD PARAMETERS
! _____
!
!l_pressure=0.0 !! 100kpa = 0.100 uN/um^2
!
! _____
!
! PROMPT FOR OTHER VALUES
! _____

*IF,MASS_RUN_FLAG,ne,1,then
  PARRES, CHANGE, '__saved_geometric_parameters','inp'
  MULTIPRO,'start'
  *CSET,1,3,g_vdpangle,'Angular Misalignment of VDP', g_vdpangle
  *CSET,4,6,XOFFSET, 'VDP offset in x (along edge)', XOFFSET
  *CSET,7,9,YOFFSETrel, 'VDP offset in y (towards center)',
YOFFSETrel
  *CSET,10,12,g_vdpsize, 'Size of VDP (in microns)', g_vdpsize
  *CSET,13,15,g_vdpdepth,'Depth of VDP (in microns)', g_vdpdepth
  *CSET,16,18,l_pressureNEW, 'Diaphragm Pressure', l_pressure
  *CSET,61,62,'Enter the values of the VDP',' position and
geometry'
```

```

*CSET,63,64,'These will be used in creating',' the submodel.'
MULTIPRO,'end'

YOFFSET=YOFFSETrel+g_basexy

      *IF, l_pressureNEW, NE, l_pressure, then
          f_ResolveDiaphragm=1
      *ELSE
          f_ResolveDiaphragm=0
      *ENDIF

l_pressure=l_pressureNEW
PARSAV, SCALAR, '__saved_geometric_parameters','inp'

      *IF, f_ResolveDiaphragm,eq,1,then
          /input,'Diaph-3D_rev8','inp',,, 0

          finish
          /clear,nostart
          /filename,'VDPsubmodel','DB',1
          /prep7

          PARRES, CHANGE, '__saved_geometric_parameters','inp'

      *ENDIF
*ENDIF

*IF,MASS_RUN_FLAG,eq,1,then
    PARRES, CHANGE, '__saved_massrun_parameters','inp'
    YOFFSET=YOFFSETrel+g_basexy
    PARSAV, SCALAR, '__saved_geometric_parameters','inp'
      *IF, f_ResolveDiaphragm,eq,1,then
          /input,'Diaph-3D_rev8','inp',,, 0

          finish
          /clear,nostart
          /filename,'VDPsubmodel','DB',1
          /prep7

          PARRES, CHANGE,
'__saved_geometric_parameters','inp'
          PARRES, CHANGE,
'__saved_massrun_parameters','inp'

      *ENDIF
*ENDIF

!
!-----
!
!   CREATE OTHER COORD SYS
!-----
!
csys,0
clocal,20,0,XOFFSET,YOFFSET,0,0,0,0

```

```

csys,20
clocal,11,0,0,0,0,g_vdpangle,0,0

csys,20
clocal,13,0,0,0,0,-45      !!! X-AXIS ALONG [1 1 0] DIR -
MATERIAL COORDS

CSYS,11
CLOCAL,12,0,0,0,0,90,0,0   ! DEFINE COORD SYS 12 FOR 90 ANGLE

CSYS,11
CLOCAL,16,0,0,0,0,90,90,0  ! DEFINE COORD SYS 16 FOR 0 ANGLE
WP (CUTS 11)

CSYS,11
CLOCAL,17,0,0,0,0,180,90,0 ! DEFINE COORD SYS 17 FOR 90 ANGLE
WP (CUTS 12)
csys,20

!
!
! MATERIAL PROPERTIES
!
!##### DEFINE PIEZORESISTIVE MATERIAL - MATERIAL 1
csys,13      ! Specify material properties:
tb,ANEL,1,,,0 ! anisotropic elasticity matrix
TBDATA,1,c11,c12,c13,0,0,0
TBDATA,7,      c11,c13,0,0,0
TBDATA,12,      c33,0,0,0
TBDATA,16,      c44,0,0
TBDATA,19,      c44,0
TBDATA,21,      c66

mp,RSVX,1,si_p_rho      ! resistivity

tb,PZRS,1      ! piezoresistive stress matrix
TBDATA,1, pi11,pi12,pi13 ,0,0,0
TBDATA,7, pi12,pi11,pi13 ,0,0,0
TBDATA,13,pi13,pi13,pi33 ,0,0,0
TBDATA,19,0,0,0, pi44,0,0
TBDATA,25,0,0,0, 0,pi44,0
TBDATA,31,0,0,0, 0,0,pi66

!
!
! RESISTOR COORDS
! & DEFINE KEYPOINTS
!
! [ CLOCAL, KCN, KCS, XL, YL, ZL, THXY, THYZ, THZX, PAR1, PAR2 ]

! CREATE RESISTOR COORD SYSTEM
csys,20

```

```

k,120,  g_submodellength/2, -g_submodelwidth/2
k,121,  g_submodellength/2,  g_submodelwidth/2
k,122, -g_submodellength/2,  g_submodelwidth/2
k,123, -g_submodellength/2, -g_submodelwidth/2

csys,12-PHI
k,130,  g_vdpsize/2, -g_vdpsize/2
k,131,  g_vdpsize/2,  g_vdpsize/2
k,132, -g_vdpsize/2,  g_vdpsize/2
k,133, -g_vdpsize/2, -g_vdpsize/2

!
!
!   DEFINE AREAS
!
!
a,120,121,122,123          ! AREA 1 - SUBMODEL AREA
a,130,131,132,133        ! AREA 2 - VDP AREA
Voffst,2,-g_vdpdepth,1000 ! VOL 1 - VDP VOLUME
voffst,1,-g_submodeldepth,2000 ! VOL 2- SUBMODEL
VOLUME
  vovlap,1,2
!
!
! DEFINE VOLUME ELEMENT
!
!
  et,1,solid227,101 ! PIEZORESISTIVE ELEMENT KEYOPT(1)=101
  et,2,solid187
!
!
! GENERATE VOLUMES - MESH
!
!
  type,1
  esys,13
  mshkey,0          ! USE MAPPED MESHING (1) FREE
MESHING (0)
  mshape,1,3D      ! USE TRIANGLE ELEMENTS (1), SQUARE
ELEMENTS (0)
  esize,g_vdpdepth/2
  mat,1
  vmesh,1

  type,2
  mat,1
  mshkey,0
  esize,g_vdpdepth*2
  esys,13
  vmesh,3
!
!

```

```

! IMPROVE VIEW
!
!
      esel,s,type,,1
      /color,elem,oran
      esel,all
      /VIEW, 1, 0.343827022543 , -0.510110968277 ,
0.788396967658
      /ANG, 1, -26.7912837612
      /REPLO

!
!
! SELECT BOUNDARY NODES FOR SUBMODELING
!
!

      csys,20
      nsel,all

      nsel,s,loc,x,-g_submodellength/2+tol,g_submodelwidth/2-tol
      nsel,r,loc,y,-g_submodellength/2+tol,g_submodelwidth/2-tol
      nsel,r,loc,z,-g_submodeldepth+tol,-tol
      nsel,inve

      nwrite,'VDPCUTBOUNDARY','NODE',,0          ! WRITE BOUNDARY NODE
FILE
      nsel,all
      save

!
!
! LOAD BOUNDARY NODES INTO DIAPHRAGM MODEL
! AND EXPORT CUR BOUNDARY DOF'S
!
!

      RESUME,'diaphragmjob','DB'
      /post1
      FILE,'diaphragmjob','rst'
      SET,1
      CBDOF,'VDPCUTBOUNDARY','NODE',,'VDPCUTBOUNDARY','CBD0',,0
      finish
      RESUME,'VDPsubmodel','DB'

      /solu

!
!
! BEGIN LOOP
! AND EXPORT CUR BOUNDARY DOF'S
!
!

      *DO,PHI,0,1                                !@@@@ LOOP ON PHI, ( 0 or 90
Orientation)

```

```

allsel,all
CSYS,20
/solu
SFDELE,all,all
DDELE,all,all
nset,all
cpdele,all

      /input,'VDPCUTBOUNDARY','CBD0'      ! APPLY CUT BOUNDARY DOF's TO
SUBMODEL

!-----
!
! APPLY SURFACE LOAD AT Z=0
!-----
!
      CSYS,12-PHI
      nsel,s,loc,z,-tol,tol
      sf,all,PRES,1_pressure
      nsel,all

!-----
!
! DELETE IMPORTED VOLTAGE CONSTRAINTS BEFORE APPLYING NEW ONES
!-----
!
      nsel,all
      ddele,all,volt
      /pbc,u,,0
      /repla

!-----
!
! ROTATE CSYS BY 90 IF PHI=1 (90deg)
! ONLY CHANGES APPLIED VOLTAGE AND MEASUREMENT LOCATIONS
!-----
!
CSYS,12-PHI
!-----
!
! APPLY VOLTAGE AT VDP CORNERS
!-----
!

VPADSIZE=0
VSPLUS=5
VSMINUS=0

nset,s,loc,x,g_vdpsize/2-VPADSIZE-tol, g_vdpsize/2+tol
nset,r,loc,y,g_vdpsize/2-VPADSIZE-tol, g_vdpsize/2+tol
nset,r,loc,z,0-tol,0+tol
!d,all,volt,5
cp,1,volt,all      ! left electrode:

```

```

*get,VSP,node,0,num,min      ! get master node
d,VSP,volt,VSPLUS           ! apply source voltage Vs
nselect,all

nselect,s,loc,x,-g_vdpsize/2-tol, -(g_vdpsize/2-VPADSIZE)+tol
nselect,r,loc,y,g_vdpsize/2-VPADSIZE-tol, g_vdpsize/2+tol
nselect,r,loc,z,0-tol,0+tol
cp,2,volt,all                ! left electrode:
*get,VSM,node,0,num,min      ! get master node
d,VSM,volt,VSMINUS          ! apply source voltage Vs
!d,all,volt,-5
nselect,all

nselect,s,loc,x,g_VDPsize/2-VPADSIZE-tol, g_VDPsize/2+tol
nselect,r,loc,y, -g_VDPsize/2-tol,-(g_VDPsize/2-VPADSIZE)+tol
nselect,r,loc,z,-tol,tol
cp,3,volt,all                ! left electrode:
*get,VOUT1,node,0,num,min    ! get master node

nselect,s,loc,x,-g_VDPsize/2-tol,-(g_VDPsize/2-VPADSIZE)+tol
nselect,r,loc,y,-g_VDPsize/2-tol,-(g_VDPsize/2-VPADSIZE)+tol
nselect,r,loc,z,-tol,tol
cp,4,volt,all                ! left electrode:
*get,VOUT2,node,0,num,min    ! get master node

nselect,all
allselect,all

!
!
!   SOLVE
!
!
!
!           /solu
!           antype,static
!           solve

!
!
!   POST PROCESS
!
!

!
!           /WAIT,1
!           /post1

!
!           plvect,JC,,,,VECT,ELEM,ON,0           ! plot current
vector

!           /PBC,volt,,1
!           /PBC,u,,0
!           /VIEW, 1, 0.343827022543, -0.510110968277,
0.788396967658
!           /ANG, 1, -26.7912837612
!           /REPLO

```

```

/WAIT,1

WPCSYS,1,17-PHI
/CPLANE,1
esel,s,type,,1
! Make CUTTING PLANE = W.

PLANE
  SUCR, SURFACE1,CPLANE,1 ! create surface
on cut plane
  SUMAP,MAPPEDJC, JC, SUM ! map vectors to
surface
  !SUPL,SURFACE1, MAPPEDJC,1 ! plot surface
mapping
  SUEVAL, INTEGRATEDCURRENT, MAPPEDJC, INTG ! Integrate
vectors on surface

WPCSYS, 1,17-PHI ! Make working plane default
CSYS,11
esel,all
nset, all

!-----
!
! OUTPUT RESULTS
!-----
!
INTEGRATEDCURRENT=INTEGRATEDCURRENT*1.0e-12
VDIFF=VOLT(VOUT1)-VOLT(VOUT2)
*IF,PHI,eq,0,then
RES_0=VDIFF/INTEGRATEDCURRENT
*ELSEIF,PHI,eq,1,then
RES_90=VDIFF/INTEGRATEDCURRENT
*ENDIF

SUDEL,all

*ENDDO !!!!! END PHI = 0 / PHI = 90 LOOP

ETABLE,TAB_SX,S,X
ETABLE,TAB_SY,S,Y

esel,all
*GET,elemcount,ELEM,0,COUNT
*GET,currelem,ELEM,0,NUM,MIN

AVG_STRESS_X=0
AVG_STRESS_Y=0
MAX_STRESS_X=0
MAX_STRESS_Y=0

*DO,loopnum,1,elemcount,1

  *GET,currstressX,ELEM,currelem,ETAB, TAB_SX
  *GET,currstressY,ELEM,currelem,ETAB, TAB_SY

```

```

*IF,abs(currstressX),gt,abs(MAX_STRESS_X),then
  MAX_STRESS_X=currstressX
*ENDIF

*IF,abs(currstressY),gt,abs(MAX_STRESS_Y),then
  MAX_STRESS_Y=currstressY
*ENDIF

AVG_STRESS_X=AVG_STRESS_X+currstressX
AVG_STRESS_Y=AVG_STRESS_Y+currstressY

*GET,currelem,ELEM,currelem,NXTH

*ENDDO
  AVG_STRESS_X=AVG_STRESS_X/elecount
  AVG_STRESS_Y=AVG_STRESS_Y/elecount

*CFOPEN, 'c:\ansyswork\3D\VDP-3Dsub_data', 'dat', ,APPEND
*VWRITE,RES_0,RES_90,g_vdpangle,XOFFSET,YOFFSETrel,g_vdpsize,g_vdpdepth
,l_pressure,AVG_STRESS_X, AVG_STRESS_Y,MAX_STRESS_X,MAX_STRESS_Y
(F12.4,F12.4,F12.4,F12.4,F12.4,F12.4,F12.4,F12.4,F12.4,F12.4,F12.4,F12.
4)
*CFCLOSE

/EOF

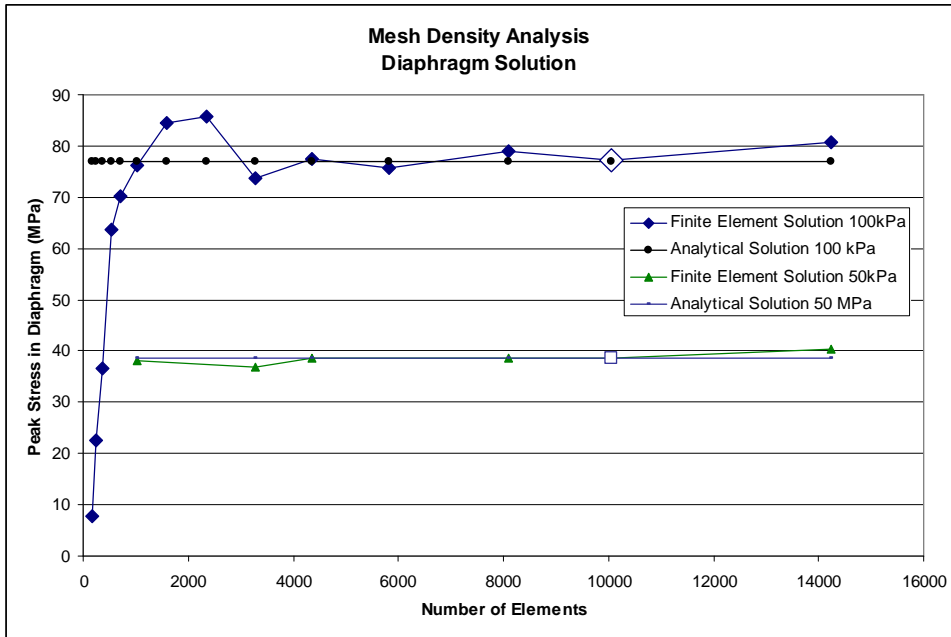
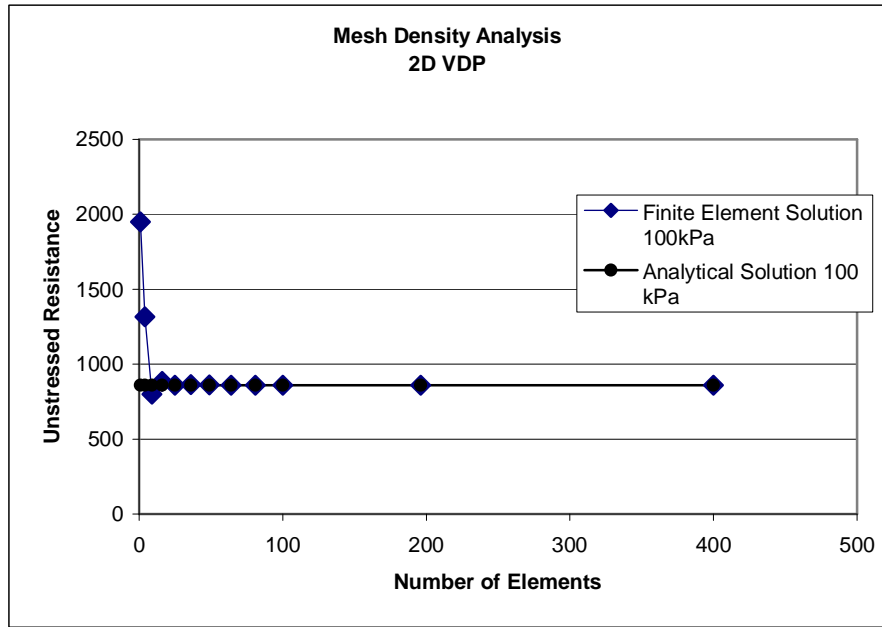
*MSG,UI, RES_0, RES_90, g_vdpangle, XOFFSET, YOFFSETrel, g_vdpsize,
g_vdpdepth,l_pressure
R_0 = %G %/&
R_90 = %G %/&
Angle = %G %/&
X offset = %G %/&
Y offset = %G %/&
VDP size = %G %/&
VDP depth = %G %/&
Pressure (MPa) = %G

*MSG,UI, AVG_STRESS_X, AVG_STRESS_Y,MAX_STRESS_X,MAX_STRESS_Y
Average X Stress = %G %/&
Average Y Stress = %G %/%/&
Maximum X Stress = %G %/&
Maximum Y Stress = %G %/

```

APPENDIX C

MESH DENSITY ANALYSES



APPENDIX D

CLAMPED PLATE SOLUTION

1) Analytical Results

TIMOSHENKO

$$w_{\max T} := 0.00126 \frac{q \cdot a^4}{D}$$

$$M_{\text{cent}T} := 0.0229 q \cdot a^2$$

$$M_{\text{edge}T} := 0.0513 q \cdot a^2$$

$$\sigma_{\text{edge}T} := \frac{6 \cdot M_{\text{edge}T}}{h^2}$$

$$\sigma_{\text{cent}T} := \frac{6 \cdot M_{\text{cent}T}}{h^2}$$

$$\sigma_{\text{edge}T} = 77.0 \text{MPa}$$

$$\sigma_{\text{cent}T} = 34.4 \text{MPa}$$

$$w_{\max T} = 17.2 \text{micron}$$

MELESHKO

$$w_{\max M} := 0.245 h \frac{q}{E} \cdot \left(\frac{0.5a}{h} \right)^4 \cdot (1 - \nu^2)$$

$$\sigma_{\text{edge}M} := 1.233 q \cdot \left(\frac{0.5a}{h} \right)^2$$

$$\sigma_{\text{edge}M} = 77.1 \text{MPa}$$

$$w_{\max M} = 17.4 \text{micron}$$

HENCKY

$$w_{\max H} := 1.265319087 \frac{q \cdot a^4}{D \cdot 1000}$$

$$M_{\text{cent}H} := 2.290509078 \frac{q \cdot a^2}{100}$$

$$M_{\text{edge}H} := 5.13337648 \frac{q \cdot a^2}{100}$$

$$\sigma_{\text{cent}H} := \frac{6 \cdot M_{\text{cent}H}}{h^2}$$

$$\sigma_{\text{edge}H} := \frac{6 \cdot M_{\text{edge}H}}{h^2}$$

$$\sigma_{\text{edge}H} = 77.0 \text{MPa}$$

$$\sigma_{\text{cent}H} = 34.4 \text{MPa}$$

$$w_{\max H} = 17.3 \text{micron}$$

*Original publisher of
approximate solution*

Peak Stress at Edge

Peak Stress at Center

**Max Displacement
at Center**

2) Series Solution

$$K := -4 \cdot \frac{q \cdot a^2}{\pi^3}$$

Setup system of simultaneous equations that arises from boundary conditions

$$A := \begin{pmatrix} 1.8033 & 0.0764 & 0.0188 & 0.0071 \\ 0.0764 & 0.4045 & 0.0330 & 0.0159 \\ 0.0188 & 0.0330 & 0.2255 & 0.0163 \\ 0.0071 & 0.0159 & 0.0163 & 0.1558 \end{pmatrix}$$

$$B := \begin{pmatrix} 0.6677 \\ 0.01232 \\ 0.00160 \\ 0.00042 \end{pmatrix} \cdot K$$

$$\alpha := \begin{pmatrix} 1 \cdot \frac{\pi \cdot b}{2 \cdot a} \\ 3 \cdot \frac{\pi \cdot b}{2 \cdot a} \\ 5 \cdot \frac{\pi \cdot b}{2 \cdot a} \\ 7 \cdot \frac{\pi \cdot b}{2 \cdot a} \end{pmatrix} \quad \beta := \begin{pmatrix} 1 \cdot \frac{\pi \cdot a}{2 \cdot b} \\ 3 \cdot \frac{\pi \cdot a}{2 \cdot b} \\ 5 \cdot \frac{\pi \cdot a}{2 \cdot b} \\ 7 \cdot \frac{\pi \cdot a}{2 \cdot b} \end{pmatrix}$$

See Timoshenko, "Theory of Plates and Shells" pp 197-202

$$Ea := \text{inv}(A) \cdot B$$

Solve system of Simulatneous equations

$$a = 0.01 \text{ m}$$

Establish Evaluation Points

$$x_{da} := \frac{-a}{2}, \frac{-a}{2} + \frac{a}{40} \dots \frac{a}{2}$$

$$y_{da} := \frac{-a}{2}, \frac{-a}{2} + \frac{a}{40} \dots \frac{a}{2}$$

Superposition solution

$$w1(x,y) := \frac{-a^2}{2\pi \cdot D} \cdot \sum_{m=0}^3 \frac{Ea_m \cdot \frac{-1}{(2m+1)^2 \cdot \cosh(\alpha_m)} \cdot \cos \left[\frac{(2m+1) \cdot \pi \cdot x}{a} \right] \cdot \left[\frac{(2m+1) \cdot \pi \cdot y}{a} \cdot \sinh \left[\frac{(2m+1) \cdot \pi \cdot y}{a} \right] - \alpha_m \cdot \tanh(\alpha_m) \cdot \cosh \left[\frac{(2m+1) \cdot \pi \cdot y}{a} \right] \right]}{(2m+1)^{-1}}$$

$$w2(x,y) := \frac{-b^2}{2\pi \cdot D} \cdot \sum_{m=0}^3 \frac{Eb_m \cdot \frac{-1}{(2m+1)^2 \cdot \cosh(\beta_m)} \cdot \cos \left[\frac{(2m+1) \cdot \pi \cdot y}{b} \right] \cdot \left[\frac{(2m+1) \cdot \pi \cdot x}{b} \cdot \sinh \left[\frac{(2m+1) \cdot \pi \cdot x}{b} \right] - \beta_m \cdot \tanh(\beta_m) \cdot \cosh \left[\frac{(2m+1) \cdot \pi \cdot x}{b} \right] \right]}{(2m+1)^{-1}}$$

$$wSS(x,y) := \frac{4 \cdot q \cdot a^4}{\pi \cdot D} \cdot \sum_{m=0}^3 \frac{1}{(2m+1)^5} \cdot \left[1 - \frac{\alpha_m \cdot \tanh(\alpha_m)}{2 \cdot \cosh(\alpha_m)} + 2 \cdot \frac{\cosh \left[\frac{2 \cdot \alpha_m(y)}{b} \right] + \frac{\alpha_m}{2 \cdot \cosh(\alpha_m)} \cdot \frac{2(y)}{b} \cdot \sinh \left[\frac{2 \cdot \alpha_m(y)}{b} \right]}{2 \cdot \cosh(\alpha_m)} \cdot \sin \left[\frac{(2m+1) \cdot \pi \cdot \left(x + \frac{a}{2} \right)}{a} \right] \right]$$

$$wtot(x,y) := -(w1(x,y) - w2(x,y) + wSS(x,y))$$

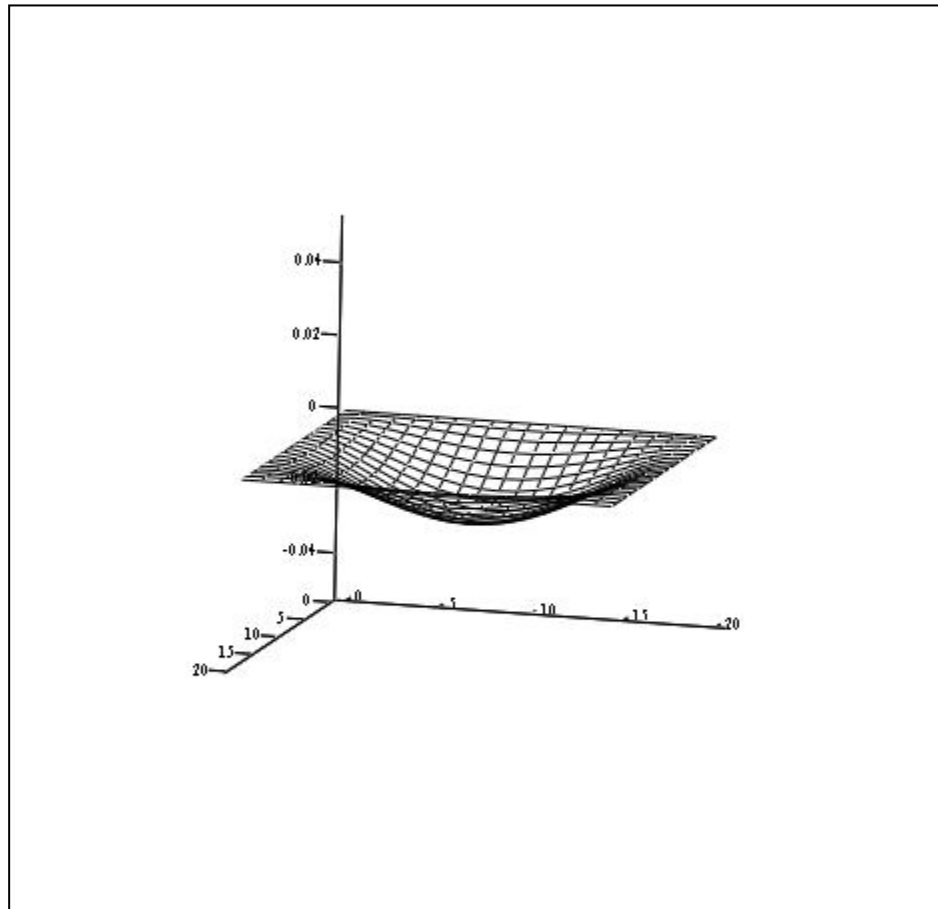
$i := 0..20$

$j := 0..20$

$$xd_i := \frac{-a}{2} + i \cdot \frac{a}{20}$$

$$yd_j := \frac{-a}{2} + j \cdot \frac{a}{20}$$

$$M_{i,j} := \text{wtot}(xd_i, yd_j) \cdot 1000$$



M

$$\sigma_x(x, y) := \frac{-E}{1 - \nu^2} \left(\frac{d^2}{dx^2} w_{\text{tot}}(x, y) + \nu \cdot \frac{d^2}{dy^2} w_{\text{tot}}(x, y) \right) \cdot \frac{h}{2}$$

$$\sigma_y(x, y) := \frac{-E}{1 - \nu^2} \left(\frac{d^2}{dy^2} w_{\text{tot}}(x, y) + \nu \cdot \frac{d^2}{dx^2} w_{\text{tot}}(x, y) \right) \cdot \frac{h}{2}$$

$$\tau_{xy}(x, y) := \frac{-E}{1 - \nu^2} \cdot \left(\frac{d}{dx} \frac{d}{dy} w_{\text{tot}}(x, y) \right) \cdot \frac{h}{2}$$

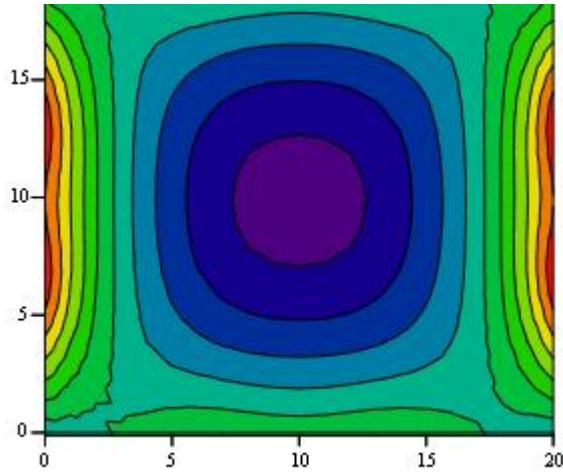
$$T_{x_{i,j}} := \sigma_x(x_{d_i}, y_{d_j})$$

$$T_{y_{i,j}} := \sigma_y(x_{d_i}, y_{d_j})$$

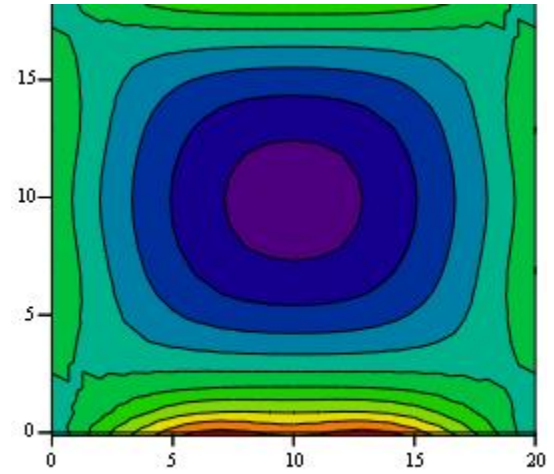
$$T_{xy_{i,j}} := \tau_{xy}(x_{d_i}, y_{d_j})$$

$$\sigma_x\left(\frac{b}{2}, 0\right) = 5.956 \times 10^7$$

$$\sigma_y\left(\frac{b}{2}, 0\right) = 1.787 \times 10^7$$



Tx

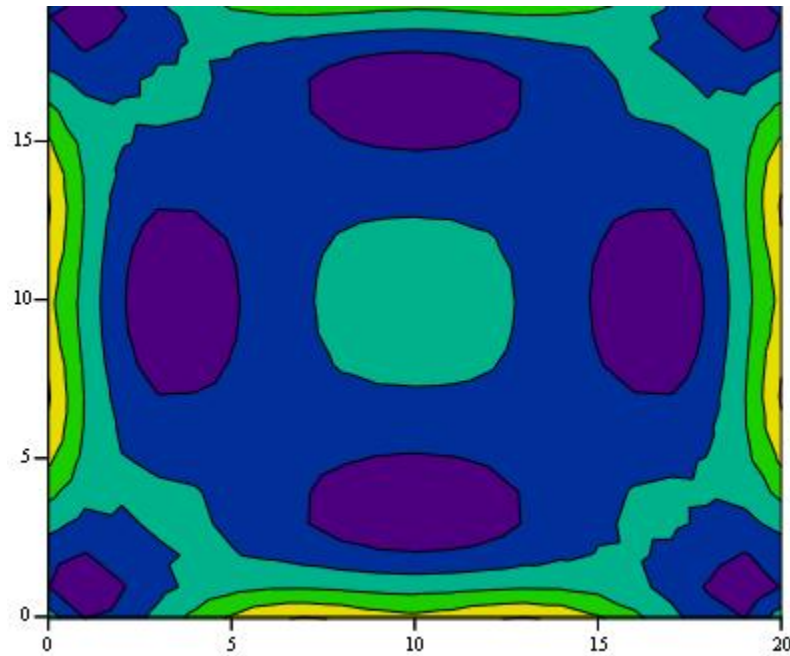
 σ_x 

Ty

 σ_y

$$\sigma_v(x, y) := \frac{1}{\sqrt{2}} \cdot \sqrt{(\sigma_x(x, y) - \sigma_y(x, y))^2 + \sigma_y(x, y)^2 + \sigma_x(x, y)^2 + 6 \cdot (\tau_{xy}(x, y))^2}$$

$$T_{v, i, j} := \sigma_v(x_{d_i}, y_{d_j})$$



T_v

von Mises stress distribution